

Bilevel subsidy-enabled mobility hub network design with perturbed utility coalitional choice-based assignment

Hai Yang^a, Joseph J. Y. Chow^{a,*}

^a*C2SMARTER University Transportation Center, Department of Civil & Urban Engineering, New York University Tandon School of Engineering, 6 MetroTech Center, Brooklyn, NY 11201, USA*

Abstract

Urban mobility is undergoing rapid transformation with the emergence of new services. Mobility hubs (MHs) have been proposed as physical-digital convergence points, offering a range of public and private mobility options in close proximity. By supporting Mobility-as-a-Service, these hubs can serve as focal points where travel decisions intersect with operator strategies. We develop a bilevel MH platform design model that treats MHs as control levers. The upper level (platform) maximizes revenue or flow by setting subsidies to incentivize last-mile operators; the lower level captures joint traveler-operator decisions with a link-based Perturbed Utility Route Choice (PURC) assignment, yielding a strictly convex quadratic program. We reformulate the bilevel problem to a single-level program via the KKT conditions of the lower level and solve it with a gap-penalty method and an iterative warm-start scheme that exploits the computationally cheap lower-level problem. Numerical experiments on a toy network and a Long Island Rail Road (LIRR) case (244 nodes, 469 links, 78 ODs) show that the method attains sub-1% optimality gaps in minutes. In the base LIRR case, the model allows policymakers to quantify the social surplus value of a MH, or the value of enabling subsidy or regulating the micro-transit operator's pricing. Comparing link-based subsidies to hub-based subsidies, the latter is computationally more expensive but offers an easier mechanism for comparison and control.

Keywords: Mobility hub, MaaS platform, Perturbed utility route choice, bilevel optimization, subsidies, assignment game

1. Introduction

Urban mobility has significantly evolved due to advances in mobile technology and digital platforms. Yet, transportation networks continue to struggle with persistent challenges including congestion, emissions, and unequal accessibility. Despite the proliferation of new mobility services like ride-hailing, car-sharing, and micromobility options, there remain challenges to fully integrate these systems to fundamentally resolve urban mobility issues. Travelers still face inconvenience in seamlessly coordinating multiple modes at transfer locations. Large proportions of commuters may still prefer driving alone if the connections to major public transit stops are inadequate or unreliable.

*Corresponding author

Email address: joseph.chow@nyu.edu (Joseph J. Y. Chow)

Emergent cyberphysical mobility hubs (MHs) are a viable response to these challenges. MHs are defined as "multimodal transport nodes that facilitate intermodal transfers by providing different mobility options in close proximity" (Miramontes et al., 2017). While "transit hubs" have existed for decades as a means to integrate land use and public transport as a type of "transit-oriented development" (see Weustenenk and Mingardo (2023)), they differ from MHs in the literature in the last decade, which feature higher levels of both physical and digital integration of mobility services (Arias-Molinares et al., 2023), particularly services that feature real-time information. These MHs often involve multiple operators (or even non-mobility-related goods and service providers, such as fueling), necessitating distinct incentives and cooperation mechanisms enabled by integrated digital platforms supporting Mobility-as-a-Service (MaaS). MaaS platforms streamline users' abilities to plan, book, and pay for various mobility services through a unified digital interface and distribute those revenues between operators, thereby aligning physical infrastructure and digital coordination. As such, MHs form critical components of cyberphysical MaaS ecosystems, acting as strategic nodes for interactions among public entities, private mobility operators, and users.

The deployment of MHs alongside MaaS schemes has been studied globally over the past decade. A notable example is the car-sharing program in Bremen, Germany (Karbaumer and Weltring, 2025). Car-sharing stations known as "mobil.punkte" are established at easily accessible locations near major public transit stops, with supporting infrastructure such as bike racks and app-based booking systems. Sustainability-focused mobility hub designs have gained more attention with the maturation of electric vehicle (EV) technologies. The eHUBS project, supported by the European Regional Development Fund, investigated the deployment of intermodal hubs focusing on electric-powered modes in six pilot cities across North-West Europe (Amsterdam, 2025). For a comprehensive review of mobility hub-focused pilot studies worldwide, readers can refer to Arnold et al. (2023).

Designing systems incorporating MHs is no trivial task. Grigolon et al. (2025) reveals that travelers are willing to pay extra to use MHs when multiple modes are easily accessible through a well-designed physical location supported by a digital platform. Existing studies predominantly focus only on their role as physical transfer points (i.e. transit hubs), where the main objective is to optimally choose the hub locations that enhance accessibility (Petrović et al., 2019; Frank et al., 2021; Aydin et al., 2022). However, these studies often overlook the potential benefits of MHs on operator strategies. For example, MHs provide a location for stationing on-demand vehicles, fueling or charging electric vehicles, and provide a means for two operators to have controlled cost transfers (i.e. only subsidize trips that start or end at MHs). For example, an integration between Long Island Railroad (LIRR) and Uber may be costly if LIRR subsidized all Uber trips to all stations, but setting boundaries for specific stations as designated MHs through bundled tickets purchased for Uber and LIRR can produce partnerships in a more cost-effective manner that can suit both parties. The problem becomes even more complex should other mobility providers wish to participate, i.e. how should LIRR consider a common platform linking with both Uber and Lyft, how should subsidies to these operators be designed, and which stations should be selected as MHs?

Effective service integration requires joint operational planning among operators to improve traveler experiences. Recent studies, such as Xanthopoulos et al. (2024), partially address this gap by considering passenger preferences in determining optimal locations and capacities of mobility hubs. Nevertheless, these works still do not fully explore how such hub characteristics as location, capacity, pricing structures, and subsidies can directly shape operators' key

decisions, including fleet allocation, service area planning, and profitability. In reality, MHs can serve as powerful control levers within public cyberphysical platforms, critically influencing both demand-side traveler choices and supply-side operator strategies. This dual influence remains largely underexplored in the current literature.

Recent advancements in MaaS modeling provide a feasible way in addressing the complex interactions between travelers and operators. Bilevel frameworks and many-to-many stable matching games (Liu and Chow, 2024; Yao and Zhang, 2024; Liu et al., 2025) have effectively captured market dynamics between travelers and operators. However, these models do not explicitly incorporate mobility hubs as integral network gateways. This gap highlights the need to systematically integrate mobility hub considerations into MaaS modeling frameworks, particularly in contexts involving complex interactions between multiple public and private operators, such as providing first-mile and last-mile services to commuter rail stations. In addition, high computational complexity associated with the MaaS models prevents larger scale deployment, which is often associated with MH design scenarios that must link both neighborhood subnetworks with larger regional subnetworks.

We fill this gap in the literature by proposing a mathematical model that optimizes the capacity allocation of shared multimodal mobility hubs while maximizing travel utility, accounting for multimodal trips and the cost transfers and subsidies between operators. In this context, operators participating in the designated MHs are part of a MaaS platform, which can be operated by a lead fixed route transit operator. To address computational complexity issues and scalability limitations inherent in existing multimodal flow assignment methods, we introduce the Perturbed Utility Route Choice (PURC)-based assignment game, based on the route choice framework from Fosgerau et al. (2022). Unlike path-enumeration approaches, the PURC framework uses link-level utilities to model dispersed multimodal route choices efficiently. This approach facilitates scalable and realistic MaaS market analyses involving mobility hubs. A case study for the neighborhoods along three LIRR stations in Suffolk County, NY, illustrates the application of the proposed mobility hub design model on a real-world scale. In addition, the case study provides valuable insights to how a MH can act as leverage in controlling the amount of subsidies used to improve transit station usage.

The paper is structured as follows. We present a literature review of the studies focusing on MH and multi-modal mobility network design games in the following section. We then explain the details of the methodology. Afterwards, we present the LIRR based case study to illustrate the model application and discuss the nuance of the service strategies involved in establishing mobility hubs. Finally, we conclude the study and discuss how the work can be extended.

2. Literature Review

Multimodal systems and mobility hub related studies cover several knowledge fields including network pricing modeling, facility location modeling, discrete choice modeling, spatial analysis, social equity evaluations, game-theory based stable matching, and many more. We do not intend to provide an exhaustive list of literature that covers all aspects of the related studies. Instead, we mainly focus on methodological works that explore the interactions among different participants when designing cooperative multimodal services (i.e. MaaS) or MH systems.

2.1. MaaS platform models

MaaS platforms integrate various transportation modes into bundles that enable more seamless trips involving multiple service operators. A MaaS platform allows users to purchase trips consisting of combinations of mobility options in a single transaction. The pricing and service schemes have attracted considerable attention in recent years (van den Berg et al., 2022). Bertsimas et al. (2020) proposed a framework that jointly optimizes schedule frequencies and service pricing in a multi-modal transit network. Given a set of multimodal trip paths, service providers optimize their service frequencies to minimize system-wide wait time under budget constraints, while passengers select their preferred routes based on a nested logit model. Hörcher and Graham (2020) compared how different MaaS subscription policies affect system performance, specifically regarding net welfare, externalities, and operator objectives. The study involves three levels of decision making: car ownership, MaaS package selection, and daily mode choice. Each level is modeled using utility maximization principles with nonlinear externalities. They found that certain pricing policies can lead to unexpected negative outcomes by encouraging the overconsumption of services.

Alternatively, two-sided market matching mechanism is adopted to model MaaS service design problems. Djavadian and Chow (2017) pioneered the two-sided market mechanism into MaaS modeling. Chen and Valant (2023) studied the convergence properties of these two-sided markets with a focus on ride-hail matching. Rasulkhani and Chow (2019) and Pantelidis et al. (2020) expanded the stable matching approach with transferable utilities to model the interaction of fixed-line service providers and travelers as a two-sided market, first as a many-to-one assignment game and then as a many-to-many assignment game. Travelers select their desired paths, which may involve multiple operators, while service operators determine whether to operate a service link and set service prices. Liu and Chow (2024) further extended this framework to incorporate mobility-on-demand (MOD) services with congested links (i.e. macroscopic matching impedance functions) for accessing MOD services. An exact solution algorithm was proposed to identify stable outcomes and determine the level of subsidy required from the platform to the operators to stabilize empty cores, highlighting the additional resources needed to operate MaaS platforms. Building on the many-to-many matching framework, Yao and Zhang (2024) proposed a different design in which the MaaS platform acts as an intermediary which purchases capacity from service providers and offers service bundles to travelers with OD-based pricing. Additionally, non-MaaS travelers are considered within the congested network.

Bilevel structures are also frequently used to formulate MaaS platform design problems. The upper level typically represents decisions made by the service platform or providers, while the lower level captures the decisions of other participants, such as travelers. Xi et al. (2024a) proposed a single-leader multi-follower game (SLMFG) in which the MaaS platform is the leader, and travelers and service providers are followers. The platform determines service bundles and pricing, while travelers and service providers choose their participation to optimize their respective objectives. Building on this work, Xi et al. (2024b) expanded the framework into a multi-leader multi-follower game (MLMFG) that considers competition among platforms in an electric MaaS (E-MaaS) ecosystem. Huang et al. (2024) used an SLMFG to model the interaction between a regulator and multiple service providers: the regulator provides path-based subsidies at the upper level, while non-cooperative service providers set link prices to maximize their own profits at the lower level. Pinto et al. (2020) adopted a bilevel structure to address a resource allocation problem, designing a multimodal system with autonomous vehicle (AV) fleets while capturing time-dependent mode choice behavior. Similarly, Bandiera et al.

(2024) formulated a bilevel problem in which service operators determine optimal strategies at the upper level and traveler behaviors are modeled at the lower level. Instead of a centralized operator, each service provider maximizes its own profit, resulting in a Nash equilibrium at the upper level.

The deterministic assignment game in (Liu and Chow, 2024; Yao and Zhang, 2024) was extended to a probabilistic approach by Liu et al. (2025) to reflect stochastic coalition choice. The assignment model adopts a similar path-based route choice framework as the capacitated SUE model from Bell (1995), but the flows reflect the joint choices of the travelers and operators on which coalitions to match. This difference from a conventional route choice model is reflected in the added operator utility term in the lower-level objective function. Because the conventional SUE model requires path-based solutions, path set generation is also a prerequisite of the solution process for the stochastic assignment game in Liu et al. (2025). However, high quality path set generation is a non-trivial task as discussed in (Prato, 2009). Furthermore, the logit-based SUE in the lower level of a bilevel optimization makes it hard to integrate into a single level problem for solving to global optimality. As such, the path-based stochastic assignment game is not well-suited for large-scale applications.

2.2. Mobility Hubs

Mobility hubs can serve as key gateways that facilitate multi-modal mobility services. However, studies related to mobility hubs mainly focus on facility location and resource allocation, i.e. aspects of traditional transit hub design in which interactions between operators are ignored. Previous research has primarily focused on locating mobility hubs to improve accessibility and reduce social inequity, with the involved facilities typically centered around a single mode. Caggiani et al. (2020a,b) proposed models to optimally place bike-share stations to enhance spatial fairness in mobility access. Similarly, Duran-Rodas et al. (2021) developed a model to site bike-share stations with the goal of minimizing spatial inequity. Other studies on hub location decisions also treat social welfare as a central research focus (Banerjee et al., 2020; Aydin et al., 2022). Frank et al. (2021) improve rural accessibility by using mobility hubs as gateways for multimodal trip itineraries. Ren and Chow (2025) integrate synthetic data with observed data to evaluate the impacts of a MH on traveler disutilities.

Although numerous models have been proposed for designing mobility hubs, only a few studies consider the interactions among mobility service participants. Nair and Miller-Hooks (2014) was a pioneer in developing hub location models that incorporate traveler mode choices. They proposed a bilevel framework, with the hub operator as the upper-level decision maker and travelers as the lower-level decision makers. Ma et al. (2019) provide a ridesharing operation strategy that prioritize interconnections with transit networks. Though not specifically designed for mobility hub application, the case study uses LIRR stations as key points for deploying proposed ridepooling dispatch and fleet repositioning strategy. The results show that the presence of a trunk commuter transit network would redistribute optimal ridepooling services to the last mile to increase effective service capacity by mitigating the "Wild Goose Chase" phenomenon (see also Ouyang and Yang (2023)). Xanthopoulos et al. (2024) also demonstrate the importance of considering user preferences in determining optimal hub locations and capacities. Their framework decomposes hub decisions and traveler choices into multiple modules, and a customized metaheuristic was developed to apply the framework at a city scale.

2.3. Research gaps and our contributions

Although numerous studies have developed models for designing multimodal service networks and mobility hubs, explicitly integrating mobility hubs into MaaS optimization frameworks remains a significant and under-explored area. Nair and Miller-Hooks (2014) and Xanthopoulos et al. (2024) captured the interaction between operator resource allocation decisions and traveler path choices. However, such analyses primarily treat hubs as mere transfer points, without explicitly considering their strategic role in operator decision-making processes. Specifically, service pricing and subsidy between operators are not considered key decision variables, even though they play crucial roles in influencing traveler choices. Xi et al. (2024a,b) proposed frameworks that leverage service capacity and pricing strategies in designing MaaS ecosystems. However, these frameworks do not consider the spatial aspects of resource allocation decisions and traveler itineraries, nor do they incorporate physical infrastructure when deciding service strategies.

The frameworks proposed by Liu and Chow (2024) and Yao and Zhang (2024) effectively capture the complex interactions among the MaaS platform, service providers, and travelers while considering flexible service strategies in multimodal networks. Nonetheless, the role of mobility hubs as key levers in MaaS ecosystem design remains unaddressed. Additionally, the above-mentioned studies often require substantial computational resources, hindering their deployments on a city-level scale. These gaps call for further modeling approaches capable of capturing strategic interactions among operators and travelers, enhanced by more scalable computational methods. A path-based stochastic assignment game approach (Liu et al., 2025) addresses some of the scalability and capturing of heterogeneous preferences, but faces others with path generation requirements.

This study addresses these gaps by rigorously integrating MH characteristics as platform control levers into MaaS market models, thereby contributing to both theoretical advancement and practical implementation strategies. The main contributions of this study are summarized as follows:

- We propose a bilevel mathematical model for the general MaaS platform design problem, given the network structure. The model aims to maximize MaaS platform revenue (if private) or social welfare (if public) while capturing the two-sided matching between mobility hub costs and traveler utility at the lower level. The upper-level decision variables are the OD-based traveler-facing pricing that grants access to the MaaS services and operator-dedicated subsidies, while the lower-level decision variables are link flows and mobility service node capacities. The proposed model involves heterogeneous operator participation and the competition mechanism, using subsidies as a lever to transfer utility between travelers and operators with heterogeneous service elements.
- We adopt a random utility model (RUM) based formulation to capture the choices of the coalitions between traveler and operator choices in the lower level as proposed by Liu et al. (2025). We extend it to a link-based formulation using the PURC approach proposed by Fosgerau et al. (2022). The approach offers improved scalability while still capturing link flows jointly determined by service operators and travelers, similar to other RUM formulations (e.g., stochastic user equilibrium, SUE).
- We reformulate the bilevel problem into a single-level problem using the Karush–Kuhn–Tucker (KKT) conditions of the lower-level problem. A gap function-based approach is proposed

to accelerate the solution process. Because of the simplicity of the PURC-based quadratic program in the lower level, a global optimum can be attained within a reasonable time frame when applied to large-scale cases.

- We apply the model to a real-world case study based on several LIRR stations and their surrounding areas to demonstrate the computational efficiency. Various operational schemes are also tested to demonstrate the impact of decisions such as pricing and subsidies. The case study provides insights for real-world policy-making in establishing mobility hubs to promote multimodal trips.

3. Proposed mobility hub platform design methodology

We first present the multimodal network structure and service assumptions. We then present the model formulations in detail. The model formulation for MH platform design takes the general stochastic MaaS assignment game from (Liu et al., 2025) and re-formulates it within an equivalent PURC framework with explicit MH decision variables. The goal is to provide a scalable framework that jointly decides the service decisions from the operator side and path choices from the customer side, while the platform sets service subsidies.

3.1. Network structure and model assumptions

The general notation for MaaS platform design used for the MH platform design follows a multicommodity network design (MCND) problem. The multimodal network G , denoted by (N, A) , consists of all nodes N and links A , serving all origin-destination (OD) and segment groups S . Origins O and destinations D are aggregated into centroids $\{O \cup D\} \subseteq N_S \subset N$. The services include a single fixed route transit (FT) operator acting as the platform for designing the MHs, and a set of MOD services that can choose to participate as feeders for these MHs through the platform. The model can be trivially modified to include fixed route buses run by other operators as feeders as well, but for simplicity in notation we assume this MH system deals only with a single fixed route platform/operator and one or more MOD feeder operators. The FT operator f belongs to a singleton set F and provides service on its own subnetwork G_f , which consists of node set $N_f \subseteq N_F \subset N$ and link set $A_f \subseteq A_F \subset A$. Similarly, each MOD fleet m belongs to the MOD operator set M , with each operating a subnetwork G_m consisting of node set $N_m \subseteq N_M \subset N$ and service link set $A_m \subseteq A_M \subset A$. A MOD service link represents a pickup at origin and drop-off at a MH, where the link attributes reflect average performance of the fleet serving this request under macroscopic modeling assumptions. Congestion effects, such as waiting for service, are captured by a node capacity at the origin. These "in-platform" links are store-and-forward links with service queues. Each MOD operator m determines the capacity for nodes $i \in N_m$, which are modeled as capacitated virtual links A_i^{\sim} to access the MOD subnetwork. The capacities are used to capture queue delays that arise from congestion while waiting for service. By representing node capacities as virtual links, we maintain a link-based network structure, ensuring consistency when estimating coefficients as per Fosgerau et al. (2022).

A dummy subnetwork is used to represent travel outside of the MH platform's multimodal services (e.g., private car, telecommuting, or an alternative platform), i.e. "out-of-platform" links. For all traveler groups S , a set of platform access and egress links A_S^+ and A_S^- are used to connect respective origins and destinations with the MH based platform. **Fig. 1** illustrates

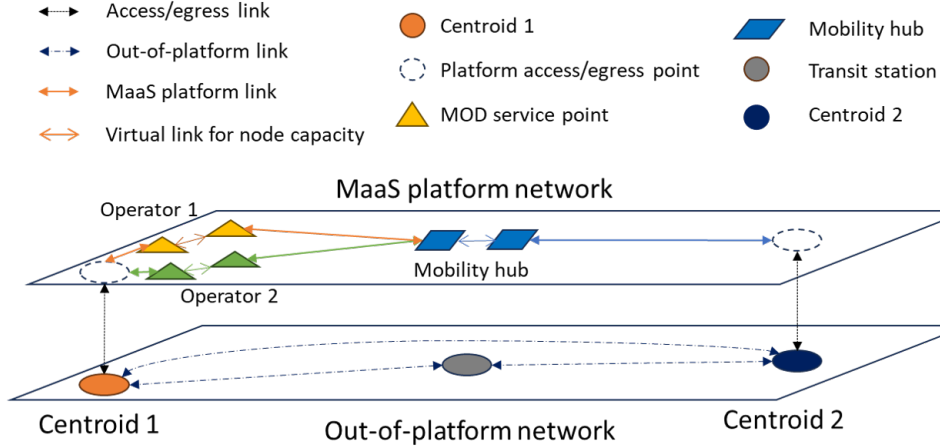


Figure 1: Network illustration for one OD pair

the multimodal network structure for one OD pair. Travelers choose their preferred paths encompassing combinations of services across the network for each OD pair segment $s \in S$, which may use the platform to access the hub and taken the fixed route transit to the destination (and vice versa), use their own modes to get to the transit station to go to the destination, or use their own mode entirely to get to the destination.

In the case of a mobility hub-oriented system, we consider a FT operator also serving as a platform regulator, working with MOD operators to provide services at designated MHs through a subset of nodes $H \subset N$. These operators may be micromobility providers, ridehail, or microtransit services. The hubs in this setting represent cyberphysical gateways in which participating MOD operators that pick up or drop off passengers purchasing trip bundles within these geofenced hubs could be subsidized. We introduce MOD feeder services centered at each hub $h \in H$, with direct access to surrounding nodes $i \in N_M$ represented by links $A_{i,h}^+$. The platform operator regulates total inbound flow to ensure it does not exceed hub capacity. For consistency, these hub capacities are modeled as virtual links A_h^\sim .

For travelers using the hub centered platform services, an OD-based access fee is charged at the access link A_s^+ for $s \in S$. After paying the access fee, traversing links belonging to the platform does not incur additional ticket charges as long as the traveler does not exit the platform-based service during the trip.

As shown in **Fig. 1**, we separate subnetworks to be "in-platform" and "out-of-platform". We focus on the OD-based pricing at the access link for travelers and service strategy decisions of operators in-platform, including operator dedicated subsidies and service capacities. Since out-of-platform includes all other options out there (including driving, walking, telecommuting, or using MOD services via pay-as-you-go option), they are assumed to be uncapacitated and we do not explicitly model competition between the designed platform and other external modes. Instead, we focus on the cooperative game between operators in-platform.

The in-platform services can be provided by multiple operators. Travelers can choose their preferred service links after entering the in-platform subnetwork by paying the access price, which is a decision variable in the model. While inside the subnetwork, only non-fee related costs are induced. For participating operators, their operating costs are covered by the subsidy provided by the platform. Other decision variables include the service capacities at either the

MH or the MOD service nodes within the in-platform subnetworks. Table 1 provides the full list of notations. In addition, we list the model assumptions as follows. To avoid confusion, we define travel cost as the non-monetary penalties associated with links such as travel time. Access price is the monetary values required for entering the in-platform subnetwork. Both terms are converted to utilities.

List of assumptions:

- The proposed model only considers strategic planning perspective. Therefore, the model only involves static flow assignment.
- The MH platforms are centrally controlled, which involves the subsidy decisions.
- All cost-related terms are link-additive.
- Utilities are transferable between travelers, operators, and the platform.
- Travel cost of the in-platform links, FT service links, and out-of-platform links are fixed.
- Transfer links between centroids and FT nodes have fixed travel cost including wait and walk time, which represent the overall cost of accessing FT services.
- MOD access links are store-and-forward links with service queues, meaning that the access flow remains uncongested until capacity is reached. Once capacity is exceeded, excess flows are diverted to other links with available capacity. The queue delay is quantified by the capacity Lagrange multiplier.
- All FT service links and links in the out-of-service subnetwork are uncapacitated. Congestion from background traffic are directly incorporated into the travel costs. If an out-of-service link reflects multiple modes, its travel cost reflects the expected minimized disutility option of those modes. Alternatively, each parallel mode may be modeled separately.
- Operating costs of MOD services consist of service link costs and access capacity allocation costs.
- Operator costs for service links, MOD nodes, and mobility hubs scale linearly with demand. We acknowledge that nonlinear functions, such as the Cobb–Douglas form (Zhang et al., 2020), are often used to capture operation cost in mobility services. However, given that this model addresses macroscopic system planning under steady-state conditions, the linear assumption provides a necessary balance between model accuracy and computational efficiency.

3.2. Lower-level traveler-operator coalition choice assignment model using PURC based structure

The MH platform design problem is adapted from the stochastic MaaS assignment game model in Liu et al. (2025). The assignment game is decomposed into a bilevel problem where the upper level involves platform decisions, such as pricing and subsidies, while the lower level involves the joint decisions of the travelers and mobility operators. In the adaptation to the MH platform design problem, the platform makes decisions about how much price to charge

Table 1: Model Variables and Parameters

Notation	Description
<i>Sets</i>	
N	Set of all nodes in the network
A	Set of all links in the network
S	Set of origin-destination (OD) pairs and population segments
$N_S \subset N$	Set of centroid nodes (OD origins/destinations)
F	Set of fixed route transit (FT) operators
$N_F \subseteq N$	Node set of all FT operators
$A_F \subseteq A$	Link set of all FT operators
$N_f \subseteq N_F$	Node set for FT operator $f \in F$
$A_f \subseteq A_F$	Link set for FT operator $f \in F$
M	Set of MOD (Mobility on Demand) operators
$N_M \subseteq N$	Node set of all MOD operators
$A_M \subseteq A$	Link set of all MOD operators
$N_m \subseteq N_M$	Node set for MOD operator $m \in M$
$A_m \subseteq A_M$	Link set for MOD operator $m \in M$
A_O	Link set for out-of-platform travel
A_0	Set of transfer links between centroids and service nodes, and between layers
$H \subset N$	Set of tentative mobility hubs
A_H	Set of added links connecting hubs and service nodes
A_h^\sim	Set of virtual hub links $h \in H$ with capacity
A_i^-	Set of outbound links of node i
A_i^+	Set of inbound links of node i
A_i^\sim	Set of virtual service node links $i \in N_M$ with capacity
$A_{i,h}^+$	Set of direct links from MOD node $i \in N_M$ to hub node h
A_S^+	Set of access links entering MH based in-platform subnetwork
<i>Input Variables (Parameters)</i>	
d_l	Length of link $l \in A$
c_l^t	Traveler cost per unit of link $l \in A$
c_l^o	Operator cost per unit of link $l \in A$
q_s	OD demand for each OD pair $s \in S$
z_l	Capacity of access links towards MOD nodes $l \in A_i^\sim, i \in N_M$
c_i	Per capacity cost of MOD node $i \in N_M$
$a_{i,l}$	Node-link incidence: -1 if node i is origin of link l , $+1$ if destination, 0 otherwise
\hat{p}_l	Cap of access price for link $l \in A_S^+$
\bar{q}	Average OD demand
α_1	Weight of traveler utility
α_2	Weight of operator utility
<i>Decision Variables</i>	
$x_{l,s}$	Normalized flow on link $l \in A$ for OD pair $s \in S$
v_l	Proportion of maximum capacity opened for access link $l \in A_{0i}$
$p_{l,s}$	Service price on platform access link $l \in A_s^+$ for each OD pair $s \in S$
r_l	Operator subsidy provided by platform based on link $l \in A_i^\sim$
b_l	Capacity of hub virtual link $l \in A_h^\sim$

travelers for each OD segment and how much to subsidize the MOD operators in the upper level, while the lower level determines the MH and MOD capacities and traveler flows.

Instead of using the path-based SUE-style formulation in Liu et al. (2025), we adapt the link-based PURC model proposed by Fosgerau et al. (2022) to capture the probabilistic matching mechanism. Eq. (1) is the link-based stochastic assignment problem L_1 based on the PURC concept for a MH platform.

$$\begin{aligned}
L_1 \min_{\{x_{l,s}, v_l\}} \Phi_1 = & \sum_{l \in A} \sum_{s \in S} \bar{q} d_l x_{l,s}^2 \\
& + \alpha_1 \bar{q} \sum_{s \in S} \left(\sum_{l \in A_s^+} d_l p_{l,s} x_{l,s} + \sum_{l \in A/A_s^+} d_l c_l x_{l,s} \right) \\
& + \alpha_2 \left(\sum_{l \in A} \sum_{s \in S} d_l c_l^o x_{l,s} q_s + \sum_{l \in A_i^{\sim}, i \in N_M} \left(z_l c_i v_l - \sum_s r_l q_s x_{l,s} \right) \right) \quad (1a)
\end{aligned}$$

$$\text{s.t. } \sum_{l \in A} a_{i,l} x_{l,s} = \begin{cases} -1, & \forall i = o, \\ 1, & \forall i = d, \\ 0, & \forall i \in N \setminus \{o, d\} \end{cases} \quad \forall s = (o, d) \in S, \forall i \in N \quad (1b)$$

$$\sum_{s \in S} x_{l,s} q_s \leq z_l v_l \quad \forall l \in A_i^{\sim}, \forall i \in N_M \quad (1c)$$

$$\sum_{l \in A_{i,h}^+} \sum_{s \in S} x_{l,s} q_s \leq b_{\tilde{l}} \quad \forall \tilde{l} \in A_h^{\sim}, \forall h \in H \quad (1d)$$

$$0 \leq x_{l,s} \leq 1 \quad \forall l \in A, \forall s \in S \quad (1e)$$

$$0 \leq v_l \leq 1 \quad \forall l \in A_i^{\sim}, \forall i \in N_M \quad (1f)$$

The assignment model Φ_1 serves as a lower level problem to the corresponding assignment game, but can also be run as an independent model for determining a multimodal network design problem with stochastic assignment, such as determining the welfare impact of an existing pricing design of a traditional transit hub without MH subsidy.

The decision variables are the percent link flow assignment $x_{l,s}$ and percent of maximum MOD service capacity v_l assigned to the access links. The platform access price $p_{l,s}$ is the decision variable in the upper level model, which is presented in the following subsection. In Φ_1 , $p_{l,s}$ is treated as an input. Eq. (1b) ensures the link flow conservation. For each OD pair $s = (o, d)$ with o being the origin and d being the destination, the source node o initiates all normalized flow, and the sink node d terminates all normalized flow. Eq. (1c) controls the capacity and congestion effect of the platform service node. All access links flowing into the service nodes are bounded by the assigned capacity the operator determines. Eq. (1d) is dedicated to mobility hub facilities. For all service flows ending at mobility hubs, the sum of flow needs to be capped by the assigned mobility hub capacity, which is determined by the platform in the upper level model. Eqs. (1e - 1f) are the bounds for the two sets of decision variables.

The objective consists of three terms: the perturbed utility, traveler utility, and the operator utility. Introduced by Fosgerau et al. (2022), the PURC model follows the general RUM structure with link-based property to capture the dispersion of flows across a network. The flow

assignment variable $x_{l,s}$ represents the probability of choosing link l for travelers in OD pair s . The first term in Eq. (1a) depicts the dispersion effect. Without this term, the model becomes an all-or-nothing assignment problem. By adding a strictly increasing function where the first and second derivatives becomes zero at the origin, a dispersion effect is added that permits deviation in route choice. Fosgerau et al. (2022) demonstrate that both quadratic and entropic functions are effective. We select the quadratic form for this study due to its simplicity, and it maintains a high level of accuracy as shown in Fosgerau et al. (2022). The second term is the sum of traveler utility, which depicts the sum of all link utilities. We simplify the term by only involving the platform access price element and general travel cost element. It can be expanded to involve all utility related elements such as externalities, as long as they can be converted to utility values. For a comprehensive explanation of the disperse effect and the utility features that can be included, readers can refer to Fosgerau et al. (2022) for more information. The original PURC objective is constructed by combining the first and second terms. We show this in **Proposition 1**.

Proposition 1. *The first and second terms combined in Eq. (1a) are equivalent to the PURC objective proposed by Fosgerau et al. (2022).*

Proof. The first and second term of Eq. (1a) can be written as Eq. (2).

$$\min_{\{x_{l,s}, v_l\}} \Phi_1 = \bar{q} \left(\sum_{l \in A} \sum_{s \in S} d_l x_{l,s}^2 + \alpha_1 \sum_{s \in S} \left(\sum_{l \in A_s^+} d_l p_{l,s} x_{l,s} + \sum_{l \in A/A_s^+} d_l c_l x_{l,s} \right) \right) \quad (2)$$

The coefficient \bar{q} is a constant. The quadratic term is the perturbed term $F(x)$, and the linear term is the link-additive utility term $U(x)$. Both terms are weighted by traversed link length d_l . The structure is therefore identical to the PURC objective proposed in Fosgerau et al. (2022) by multiplying with a constant \bar{q} . \square

We introduce the third term to form the coalition between travelers and operators in a similar fashion to the model proposed by Liu et al. (2025). In **Proposition 2**, we show that Φ_1 provides a flow assignment model with a traveler-operator coalition under the rule of PURC.

Proposition 2. Φ_1 *yields the link flow assignment under PURC framework with traveler and operator coalition choice.*

Proof. We divide Eq. (1a) by the constant term \bar{q} and write it as Eq. (3).

$$\begin{aligned} \min_{\{x_{l,s}, v_l\}} \Phi'_1 &= \sum_{l \in A} \sum_{s \in S} d_l x_{l,s}^2 \\ &+ \alpha_1 \sum_{s \in S} \left(\sum_{l \in A_s^+} d_l p_{l,s} x_{l,s} + \sum_{l \in A \setminus A_s^+} d_l c_l x_{l,s} \right) \\ &+ \alpha_2 \left(\sum_{l \in A} \sum_{s \in S} d_l c_l^o x_{l,s} \frac{q_s}{\bar{q}} + \sum_{l \in A_i^{\sim}} \frac{z_l c_l v_l - \sum_s r_l q_s x_{l,s}}{\bar{q}} \right) \end{aligned} \quad (3)$$

The Lagrangian of Φ'_1 is written as Eq. (4).

$$\begin{aligned}
\min_{\{x_{l,s}, v_i\}} L'_1 = & \sum_{l \in A} \sum_{s \in S} d_l x_{l,s}^2 \\
& + \alpha_1 \sum_{s \in S} \left(\sum_{l \in A_s^+} d_l p_{l,s} x_{l,s} + \sum_{l \in A \setminus A_s^+} d_l c_l x_{l,s} \right) \\
& + \alpha_2 \left(\sum_{l \in A} \sum_{s \in S} d_l c_l^o x_{l,s} \frac{q_s}{\bar{q}} + \sum_{l \in A_i^\sim} \frac{z_l c_i v_l - \sum_s r_l q_s x_{l,s}}{\bar{q}} \right) \\
& + \sum_{s \in S} \sum_{i \in N} \mu_{i,s} \left(\sum_l a_{i,l} x_{l,s} - f_{i,s} \right) \\
& + \sum_{l \in A_i^\sim, i \in N_M} \lambda_l \left(\sum_{s \in S} x_{l,s} q_s - z_l v_l \right) \\
& + \sum_{\tilde{l} \in A_h^\sim, h \in H} \varphi_{\tilde{l}} \left(\sum_{l \in A_{i,h}^+} \sum_{s \in S} x_{l,s} q_s - b_{\tilde{l}} \right) \\
& + \sum_{l \in A} \sum_{s \in S} \beta_{l,s} (x_{l,s} - 1) + \sum_{l \in A_i^\sim, i \in N_M} \pi_l (v_l - 1)
\end{aligned} \tag{4}$$

The optimal solution of $x_{l,s}$ is obtained by having $\frac{\partial L'_1}{x_{l,s}} = 0$ for all chosen links l for OD pair s .

$$\begin{aligned}
\frac{\partial L'_1}{x_{l,s}} = & 2d_l x_{l,s} + d_l \left(\alpha_1 (p_l + c_l) + \alpha_2 \frac{(c_l^o - r_l) q_s}{\bar{q}} \right) \\
& + \sum_{i \in l^+, l^-} \mu_{i,s} a_{i,l} + \lambda_l q_s + \sum_{\tilde{l}^- \in l^+} \varphi_{\tilde{l}} q_s + \beta_{l,s} = 0
\end{aligned} \tag{5}$$

We slightly change the notation of the term associated with α_1 in Eq. 5 for simplicity. By setting c_l to zero when $l \in A_s^+$ and p_l to zero when $l \in A \setminus A_s^+$, Eq. 5 is equivalent to the first order derivative of Eq 4. Because the chosen links will have strictly positive flows, the v_l associated with those links also fulfill the optimality conditions.

$$\frac{\partial L'_1}{v_l} = \alpha_2 \frac{z_l c_i}{\bar{q}} - \lambda_l z_l + \pi_l = 0 \tag{6}$$

By re-writing Eq. (6), we obtain $\lambda_l = \frac{\alpha_2 c_i}{\bar{q}} + \frac{\pi_l}{z_l}$. By plugging it in Eq. (5), we have Eq. (7).

$$\frac{\partial L'_1}{x_{l,s}} = 2d_l x_{l,s} + d_l \left(\alpha_1 (p_l + c_l) + \alpha_2 \frac{(c_l^o - r_l) q_s}{\bar{q}} \right) \tag{7a}$$

$$+ \sum_{i \in l^+, l^-} \mu_{i,s} a_{i,l} + \sum_{i \in l^+} \alpha_2 c_i \frac{q_s}{\bar{q}} + \frac{\pi_l q_s}{z_l} + \sum_{l' \in l^+} \varphi_{l'} q_s + \beta_{l,s} = 0 \tag{7b}$$

Eq. (7) can be rewritten as Eq. (8).

$$x_{l,s} = -\frac{1}{2} \left(\alpha_1 (p_l + c_l) + \alpha_2 \frac{(c_l^o - r_l) q_s}{\bar{q}} \right) - \frac{1}{2d} \left(\sum_{i \in l^+, l^-} \mu_{i,s} a_{i,l} + \sum_{i \in l^+} \alpha_2 c_i \frac{q_s}{\bar{q}} + \frac{\pi_l q_s}{z_l} + \sum_{l' \in l^+} \varphi_{l'} q_s + \beta_{l,s} \right) \quad (8)$$

Eq. (8) depicts the flow assignment decisions for all links l with positive flows for each OD pair s . The first term consists of the link disutility from both travelers and operators. The link disutilities from the two sides are weighted by α_1, α_2 , and q_s/\bar{q} . α_1 and α_2 are traveler and operator dedicated coefficients that provide different weights towards the overall utility objective. The ratio of α_1/α_2 depicts which side having higher impact towards the flow assignment behavior. q_s/\bar{q} is an additional weight that considers the impact from different OD pair volumes. The flow assignment variable $x_{l,s}$ is considered as the possibility of choosing link l for OD group s . Each OD pair shall be treated equally from a traveler perspective to reflect stochastic user-equilibrium (SUE) behavior from the perspective of the coalitions of travelers and operators. The weight q_s/\bar{q} is the lever that places more focus on OD pairs with higher OD volume.

The second term consists of node and capacity specific values. The first element represents the magnitude of attraction of link l in OD pair s , which is measured by the difference between the source and sink node Lagrange multipliers. The second element represents the disutility from the cost of serving a node for MOD operators. For links that do not belong to the access link set leading to MOD nodes N_M , the second element is dropped. For the the access links leading to MOD nodes, the node cost disutility from the operator side is counted towards the flow assignment, which is also weighted by q_s/\bar{q} . The remaining three terms are the Lagrange multipliers associated with MOD service node capacity, hub capacity, and link flow constraints.

Eq. (8) mimics the structure of the optimal link-flow decision variable with non-zero value shown in Fosgerau et al. (2022). This concludes the proof. \square

Representing the differences in the joint behavior of the traveler and operator coalitions, α_1 and α_2 would typically be fitted to data in practice to help regulate the dispersion effect observed in the data. As shown in Fosgerau et al. (2022), route dispersion intensifies when the first term in Eq. (1a) holds greater relative weight. If the observed flows have less divergent route choice behavior, the magnitudes of α_1 and α_2 can be both raised while maintaining the same ratio of α_1/α_2 .

Bell (1995) proved that the congestion effect can be reflected by the capacity Lagrange multiplier in a capacitated network, which is also shown in Liu et al. (2025). We follow the same logic to show that the congestion effect can also be evaluated by capacity Lagrange multipliers in the PURC based assignment model.

Proposition 3. *The congestion effect of waiting for service at a capacitated MOD access link $l \in A_i^{\sim}, i \in N_M$ is captured by the corresponding Lagrange multiplier λ_l . Similarly, the congestion effect caused by the capacitated hub facility $l \in A_h^{\sim}, h \in H$ is captured by the corresponding Lagrange multiplier φ_l .*

Proof. We use the congestion effect at MOD access links as an example. Assume an access link l with sink node i is at capacity ($v_l = 1$). If there is an additional flow δ_s for OD pair s on link l , the capacity constraint Eq. (1c) is therefore exceeded by $\frac{\delta_s q_s}{z_l}$. Assume the additional flow switches to link l' while the chosen downstream links have identical costs compared to the

chosen downstream links sourcing from node i . The change of objective value measured by Eq. (1a) is written as Eq. (9).

$$d\Phi_1 = \bar{q}(d_l(2x_{l,s} + \delta_s) - d_{l'}(2x_{l',s} + \delta_s)) + \bar{q}\delta_s(d_l p_l - d_{l'} p_{l'} + d_l c_l^t - d_{l'} c_{l'}^t) + \alpha \delta_s(d_l c_l^o - d_{l'} c_{l'}^o) q_s \quad (9)$$

As shown in Eq. (10), when the right-hand side of the node capacity constraint Eq. (1f) increases by 1, the objective value of the KKT in Eq. (4) increases by π_l . Therefore, we can rewrite Eq. (9) as Eq. (11).

$$\frac{d\Phi_1}{\delta_s q_s / z_l} = \frac{z_l \bar{q}}{q_s} (d_l(2x_{l,s} + \delta_s) - d_{l'}(2x_{l',s} + \delta_s)) + \frac{z_l \bar{q}}{q_s} (d_l p_l - d_{l'} p_{l'} + d_l c_l^t - d_{l'} c_{l'}^t) + \alpha z_l (d_l c_l^o - d_{l'} c_{l'}^o) = \pi_l \quad (10)$$

$$\frac{\bar{q}}{q_s} (d_l(2x_{l,s} + \delta_s) - d_{l'}(2x_{l',s} + \delta_s)) + \frac{\bar{q}}{q_s} (d_l p_l - d_{l'} p_{l'} + d_l c_l^t - d_{l'} c_{l'}^t) + \alpha (d_l c_l^o - d_{l'} c_{l'}^o) = \frac{\pi_l}{z_l} \quad (11)$$

If link l and l' both having 1 unit of length, Eq. (11) is equivalent to Eq. (12).

$$x_{l,s} - x_{l',s} = -(p_l - p_{l'}) - (c_l^t + \frac{\pi_l q_s}{z_l \bar{q}} - c_{l'}^t) - \alpha (c_l^o - c_{l'}^o) \frac{q_s}{\bar{q}} \quad (12)$$

Eq. (12) shows that the congestion effect caused by the capacitated node can be evaluated by the Lagrange multiplier of the node capacity constraint. When the switched links are identical in length, the congestion effect equals to $\frac{\pi_l q_l}{z_l \bar{q}}$. The same logic can be applied to capacitated hub links. This concludes the proof. \square

The lower-level assignment model is a convex quadratic programming (QP) problem, which can be easily solved with off-the-shelf solvers at scale. Moreover, it exhibits characteristics that allow us to solve the bilevel problem to global optimality as well.

3.3. Upper level model formulation

We present the upper-level problem in this subsection. The decision-maker of the upper-level problem is the MH platform, which determines the optimal OD-based pricing strategy for accessing the mobility service, the capacity assigned to hub locations, and the subsidy provided to incentivize operator participation. The bilevel structure follows the Stackelberg equilibrium principle, with the MaaS platform as the leader that sets pricing, capacity, and subsidy decisions, while travelers and operators are followers who make decisions to minimize their disutilities. We use revenue maximization as the upper-level objective. However, other equity or social welfare focuses objective can be applied for the upper level objective. From a revenue maximization perspective, the mobility hub design problem can be formulated as Eq. (13).

$$\max_{\mathbf{p}, \mathbf{r}, \mathbf{b}} \Phi_0 = \sum_s \sum_{l \in A_s^+} p_s x_{l,s} q_s - \sum_{l \in A_H} \sum_{i \in l^-} c_i b_l - \sum_{m \in M} \sum_{i \in N_m} \sum_{l \in A_i^{\sim}} \sum_{s \in S} r_l x_{l,s} q_s \quad (13a)$$

$$\text{s.t. } \mathbf{x} = \arg \min_{\mathbf{x}} \Phi_1(\mathbf{p}, \mathbf{r}, \mathbf{b}) \quad (13b)$$

$$0 \leq p_s \leq \hat{p}, \quad \forall s \in S \quad (13c)$$

$$0 \leq b_l \leq \hat{b}, \quad \forall l \in A_H \quad (13d)$$

$$0 \leq r_l \leq \hat{r}, \quad \forall l \in A_i^{\sim}, \forall i \in N_M \quad (13e)$$

$$\sum_{i \in N_m} \sum_{l \in A_i^{\sim}} \sum_{s \in S} r_l x_{l,s} q_s - \sum_{l \in A_m} \sum_{s \in S} d_l c_l^o x_{l,s} q_s - \sum_{i \in N_m} \sum_{l \in A_i^{\sim}} z_l c_i v_l \geq 0, \quad \forall m \in M \quad (13f)$$

The upper-level problem finds the optimal pricing strategy, along with the hub capacity and operator subsidy, that maximize the total revenue of the MH platform, while the service flows and MOD route capacities are determined by the lower-level problem. The first and second terms represent the total income from passenger access and the hub operating cost. The third term represents the total subsidy provided to participating MOD operators. The model assumes that \hat{p} , \hat{b} , and \hat{r} reflect the existing conditions that the market accepts. These parameters could be further segmented for specific traveler and operator groups. We adopt uniform, system-wide values for simplicity in Eq. (13c - 13e). Eq. (13f) requires that the subsidy for each MOD operator cover the operating cost so participation in the MH-oriented platform is profitable.

We can also slightly modify the objective so that subsidy also comes from outside resources (e.g., local authority). Assuming there is a fixed subsidy package R provided to the platform operator, then by directly adding R to Eq. (13a), we can effectively capture the impact of outside subsidy without modifying the constraints.

Aside from the PURC modifications, the bilevel problem presented in these two subsections feature several nontrivial differences from the generic MaaS assignment game model from (Liu and Chow, 2024) and (Liu et al., 2025). These include:

- In-platform links only include the ones inbound and outbound from MHs; the consequence is the capacity designs focus only on which last-mile service regions the MOD operators would serve (capacities approaching zero suggests not serving those regions) and the capacities for the MHs (capacities approaching zero here suggests closing the MH).
- There are out-of-platform links not just connecting centroid OD pairs, but also connecting centroids to the FT operators' stations as out-of-platform access links for travelers choosing to use the FT service without engaging with the platform.
- Whereas the stochastic assignment game in (Liu et al., 2025) lacks a subsidy and the deterministic one in (Liu and Chow, 2024) only subsidizes a system that has no stable outcome otherwise, the proposed model determines both price and subsidy as upper-level decisions with a guaranteed stable outcome. As shown in Liu et al. (2025), the stochastic assignment game is guaranteed to have a stable outcome with a single cost allocation corresponding to the optimal flow because of the endogeneity in the coalition choices. The added subsidy further assures the participating operator's profitability while strictly following the coalition structure, making the model more applicable in real-world adaptation.
- The general MaaS platform assignment game assumes there is no preexisting network, so as costs for operators go up, the optimal solution will have everybody move to out-of-platform alternatives. In the proposed model, there is a preexisting FT service, so if costs of operating MHs are too high, out-of-platform flows imply travelers either going to their destinations or to the transit stations on their own modes via driving, walking, or pay-as-you-go options.

3.4. Solution method

The bilevel programming problem is nonconvex due to the dependency between leader and follower. The bilevel problem can be reformulated into a single-level constrained optimization problem by incorporating the KKT conditions of Eq. (1) as additional constraints into Eq. (13). The reformulated single-level problem is written as Eq. (14).

$$\max_{\mathbf{p}, \mathbf{x}, \mathbf{v}, \mu, \lambda, \beta, \pi} \Phi'_0 = \sum_s \sum_{l \in A_s^+} p_s x_{l,s} q_s - \sum_{l \in A_H} \sum_{i \in l^-} c_i b_l - \sum_{m \in M} \sum_{i \in N_m} \sum_{l \in A_i^-} \sum_{s \in S} r_l x_{l,s} q_s \quad (14a)$$

$$\text{s.t. } 0 \leq p_s \leq \hat{p}, \quad \forall s \in S \quad (14b)$$

$$0 \leq b_l \leq \hat{b}, \quad \forall l \in A_H \quad (14c)$$

$$0 \leq r_l \leq \hat{r}, \quad \forall l \in A_i^-, \forall i \in N_M \quad (14d)$$

$$\sum_{i \in N_m} \sum_{l \in A_i^-} \sum_{s \in S} r_l x_{l,s} q_s - \sum_{l \in A_m} \sum_{s \in S} d_l c_l^o x_{l,s} q_s - \sum_{i \in N_m} \sum_{l \in A_i^-} z_l c_i v_l \geq 0, \quad \forall m \in M \quad (14e)$$

$$x_{l,s} (2d_l x_{l,s} + d_l \left(\alpha_1 (p_l + c_l) + \alpha_2 \frac{(c_l^o - r_l) q_s}{\bar{q}} \right) + \sum_{i \in l^+, l^-} \mu_{i,s} a_{i,l} + \sum_{i \in l^+} \alpha_2 c_i \frac{q_s}{\bar{q}} + \sum_{l' \in l^+} \varphi_{l'} q_s + \beta_{l,s}) = 0 \quad \forall l \in A, \forall s \in S \quad (14f)$$

$$\alpha_2 \frac{z_l c_i}{\bar{q}} - \lambda_l z_l + \pi_l = 0, \quad \forall l \in A_i^-, \forall i \in N_M \quad (14g)$$

$$\mu_{i,s} \left(\sum_l a_{i,l} x_{l,s} - f_{i,s} \right) = 0, \quad \forall i \in N, \forall s \in S \quad (14h)$$

$$\lambda_l \left(\sum_{s \in S} x_{l,s} q_s - z_l v_l \right) = 0 \quad \forall l \in A_i^-, \forall i \in N_M \quad (14i)$$

$$\varphi_{\tilde{l}} \left(\sum_{l \in A_{i,h}^+} \sum_{s \in S} x_{l,s} q_s - b_{\tilde{l}} \right) = 0, \quad \forall \tilde{l} \in A_h^-, \forall h \in H \quad (14j)$$

$$\beta_{l,s} (x_{l,s} - 1) = 0, \quad \forall l \in A, s \in S \quad (14k)$$

$$\pi_l (v_l - 1) = 0, \quad \forall l \in A_i^-, \forall i \in N_M \quad (14l)$$

$$\sum_{l \in A} a_{i,l} x_{l,s} = \begin{cases} -1, & \forall i = o, \\ 1, & \forall i = d, \\ 0, & \forall i \in N \setminus \{o, d\} \end{cases} \quad \forall s = (o, d) \in S, \forall i \in N \quad (14m)$$

$$\sum_{s \in S} x_{l,s} q_s \leq z_l v_l \quad \forall l \in A_i^-, \forall i \in N_M \quad (14n)$$

$$\sum_{l \in A_{i,h}^+} \sum_{s \in S} x_{l,s} q_s \leq b_{\tilde{l}} \quad \forall \tilde{l} \in A_h^-, \forall h \in H \quad (14o)$$

$$\mathbf{p}, \mathbf{x}, \mathbf{v}, \mu, \lambda, \beta, \pi \geq 0 \quad (14p)$$

Eqs. (14f, 14g) are the first order conditions. Eq. (14f) is an augmented first order condition because of the zero-flow links involved in the final solution as indicated in Fosgerau et al. (2022). Eqs. (14h - 14l) are the complementarity slackness conditions. It has been shown (e.g. Dempe (2002)) that bilevel problems with linear upper level and convex quadratic lower level programs can be reformulated into a single level mathematical program with complementarity

constraints (MPCC) that can be solved to global optimality. Sinha et al. (2017) provide an example algorithm based on branch-and-bound.

However, the added KKT multipliers and complementarity constraints pose great scalability challenges, especially when facing a large network. Therefore, it is impractical to solve for a global optimal solution using branch-and-bound. To address this issue, we adopt the gap function-based method proposed by Marcotte and Zhu (1996) to solve the bilevel problem effectively while still keeping high solution quality. Instead of directly appending the KKT conditions into upper-level constraints, we move part of the high-dimension constraints into the objective function and formulate them as penalty terms. The new penalty added objective and the adjusted constraints are written as Eq. (15).

$$\min_{\mathbf{p}, \mathbf{x}, \mathbf{v}, \mu, \lambda, \beta, \pi} \Phi'_0 = - \sum_s \sum_l d_l p_l x_{s,l} q_s + \rho \sum_{l,s} \Lambda_{l,s} \quad (15a)$$

$$\text{s.t. } \Lambda_{l,s} \geq 0, \quad \forall l \in A, s \in S \quad (15b)$$

$$\text{Eqs. (14b-14d, 14g-14p)} \quad (15c)$$

The penalty term $\Lambda_{l,s}$ is the augmented first order condition Eq. (14f) for each l, s pair. The penalty coefficient ρ is a tunable hyperparameter that modifies the magnitude of the penalty. The higher the value of ρ , the heavier the penalty when not solved towards the lower-level optima. When ρ is sufficiently high, Eq. (15) is equivalent to minimizing the upper level objective while obtaining the lower level optimum. Therefore, we can also solve Eq. (15) to obtain a global optimum of this bilevel problem.

Proposition 4. *There exists a value of ρ for which the solution obtained from solving Eq. (15) converges to the optimal solution obtained from Eq. (14).*

Proof. The equality constraint Eq. (14f) can be written as Eq. (16).

$$\Lambda_{l,s} \geq 0, \quad \forall l \in A, s \in S \quad (16a)$$

$$\Lambda_{l,s} \leq 0, \quad \forall l \in A, s \in S \quad (16b)$$

We denote the Lagrangian multiplier of Eq. (16b) to be $\eta_{l,s}$. We switch the original objective Eq. (14a) to a minimization problem. We then relax Eq. (16b) to have Eq. (17).

$$\min - \sum_s \sum_l d_l p_l x_{s,l} q_s + \sum_{l,s} \eta_{l,s} \Lambda_{l,s} \quad (17a)$$

$$\Lambda_{l,s} \geq 0, \quad \forall l \in A, s \in S \quad (17b)$$

When $\rho \geq \max(\eta)$, the penalty term $\rho \sum \Lambda$ dominates the incentive to violate Eq. (16b). Under this condition, any optimal solution of the original problem is optimal for the penalized problem. The equality constraint Eq. (14f) is recovered at the optimum even though the feasible set only enforces Eq. (17b). This completes the proof. \square

To further reduce the computational load, we propose another algorithmic improvement. Since the lower-level problem is very efficient to solve due to its convexity, it is easy to obtain the lower-level optimum when \mathbf{p} and \mathbf{r} are fixed. We use an iterative update process to exploit

this property and reduce the solution time for Eq. (15). The overall proposed algorithm is summarized in **Algorithm 1**. The hyperparameters ρ^0 , ψ^- , and ψ^+ control the rate of penalty update, where $\psi^+ > 1$ and $\psi^- < 1$. By starting with a small value ρ^0 , Eq. (15) is easier to solve to optimality. This comes with the cost of violating lower-level KKT condition by a large margin ($\sum \Lambda \gg \epsilon$). By gradually increasing ρ with ψ^+ , the KKT violation shrinks, leading to the global optimum. However, when ρ becomes too large, the single-level solution process can become computationally intensive. Therefore, we reduce ρ by ψ^- to control the step size. Within each iteration, the previously solved \mathbf{p} and \mathbf{r} are used to solve the lower-level problem first. This solution, along with all dual values and their bounds, can warm-start the single-level solution algorithm in a tighter space, leading to a shorter runtime. After meeting the convergence criteria or reaching the maximum number of iterations, we output the final values of $(\mathbf{p}^*, \mathbf{r}^*, \mathbf{x}^*, \mathbf{v}^*)$.

Algorithm 1 Penalty-Based Iterative Solution Method for Mobility Hub Platform Design Problem

- 1: **Input:** Initial upper-level variable $\mathbf{p}^0, \mathbf{r}^0$, initial penalty parameter ρ^0 , bound relaxation coefficient ζ , penalty parameter update coefficient ψ^-, ψ^+ , optimality gap target τ , objective tolerance ϵ , time limit T , maximum iterations K
 - 2: $k \leftarrow 0$
 - 3: **repeat**
 - 4: **Step 1:** For given $\mathbf{p}^k, \mathbf{r}^k$, solve the lower-level problem Eq. (1) to obtain optimal $\mathbf{x}^k, \mathbf{v}^k$
 - 5: **Step 2:** Obtain all Lagrangians $\lambda^k, \mu^k, \beta^k, \pi^k$ from the lower level solutions and their current bounds.
 - 6: **Step 3:** Load and warm start the solution process for Eq. (15) using $\mathbf{x}^k, \mathbf{v}^k, \lambda^k, \mu^k, \beta^k, \pi^k$ and ρ^k . Update the bounds for $\lambda^k, \mu^k, \beta^k, \pi^k$ by ζ . Solve until time limit T is reached or the optimality gap is lower than τ . Obtain the new solution \mathbf{p}, \mathbf{r} .
 - 7: **Step 4:** Check optimality condition:
 - 8: **if** Optimality gap $\leq \tau$ **then**
 - 9: Go to step 5
 - 10: **else**
 - 11: $\rho^k \leftarrow \psi^- \rho^k$
 - 12: **end if**
 - 13: **Step 5:** Check penalty condition:
 - 14: **if** $\sum \Lambda \leq \epsilon$ **or** $k \geq K$ **then**
 - 15: **Break**
 - 16: **else**
 - 17: $\rho^k \leftarrow \psi^+ \rho^k$
 - 18: **end if**
 - 19: **Step 6:** $\mathbf{p}^k, \mathbf{r}^k = \mathbf{p}, \mathbf{r}$
 - 20: $k \leftarrow k + 1$
 - 21: **until** convergence
 - 22: Solve lower level problem Eq. (1) with $\mathbf{p}^*, \mathbf{r}^*$. Obtain $\mathbf{x}^*, \mathbf{v}^*$
 - 23: **Output:** Optimal solution $(\mathbf{p}^*, \mathbf{r}^*, \mathbf{x}^*, \mathbf{v}^*)$.
-

4. Numerical experiments

In this section, we provide two sets of experiments to illustrate the formulation and the solution algorithm. We first use a toy network to verify the algorithm and illustrate the model. The second experiment is tested on a hypothetical multimodal network centered around three LIRR stations, which serve as potential mobility hubs for travelers commuting to New York City from Long Island.

4.1. Illustrative example

A toy network is illustrated in **Fig. 2**. Three OD pairs are considered: $(1, 0)$, $(2, 0)$, and $(3, 0)$, each with a demand of 100 units over a typical operating period. The MaaS platform is considered for the transit line from mobility hub H to node $0'$, as well as MOD service links from nodes 1, 2, and 3 to node H. For node 1, two MOD service options are provided (e.g., car sharing and micromobility) with different cost attributes for both travelers and operators. The gray dotted links represent out-of-platform services (e.g., privately owned vehicles, walking, or other pay-as-you-go services). All platform-based nodes A, B, C, D, and H have virtual links to represent node capacities. Nodes A, B, and C are operated by the car sharing company (denoted as MOD 1) and node D is operated by the micromobility company (denoted as MOD 2). Both the MH node and MOD service nodes have capacity constraints and associated capacity costs. The MH capacity reflects the supply-side resources for supporting a fleet there: dedicated space for temporary stationing, maintenance, fueling, etc. The service node capacity reflects the availability constraint and the associated service stop establishment cost. For each OD pair, dedicated platform access links are defined for traveler pricing purposes.

Core input parameters are listed in **Table 2**. All access, egress, and virtual capacity links are assigned a small length value, which is used to prevent infeasible solutions without impacting the flow assignment results. Virtual node capacity links have zero cost and price and are also assigned a small length value to prevent infeasibility. The three MOD access links $(1 - 1')$, $(2 - 2')$, $(3 - 3')$ are controlled by the platform to adjust suitable service pricing in the upper-level problem along with operator-facing subsidies assuring operator profitability. Other services have fixed costs. c_i^t , c_i^o , and p_i are all measured in monetary values. We want to highlight that after paying the access fee when traversing link $1 - 1'$, travelers from node 1 are free to choose either $1' - A$ or $1' - D$ without additional fare cost, which reflects the "bundled" feature of such a platform. Such behavioral decisions are determined by the lower-level problem, which decides the joint choice of traveler flow and hub capacities.

The toy example is solved on a device with an Intel(R) i7-13705 processor. We directly solve it to global optimality using Gurobi 12.1 and the branch-and-bound algorithm, with the optimality gap being less than 10^{-4} . All scenarios reach the global optimum under 1 second.

The results are summarized in **Table 3** under the columns "Price", "Subsidy", and "Flow". Flows on virtual capacity links (e.g., D-D') are not shown in the table for simplicity. OD pair $(3, 0)$ relies exclusively on the direct non-MaaS link, whereas OD pairs $(1, 0)$ and $(2, 0)$ exhibit multimodal routing behavior, combining both direct and MaaS-integrated links. Specifically, flows for OD $(1, 0)$ and $(2, 0)$ are distributed across three routes: the direct link, a non-MaaS path using the transit connection, and a MOD-only path. This highlights the benefits to travelers starting from nodes 1 and 2 when MOD services are introduced. However, under the provided pricing scheme for OD $(1, 0)$, no travelers select service node A, and the service link

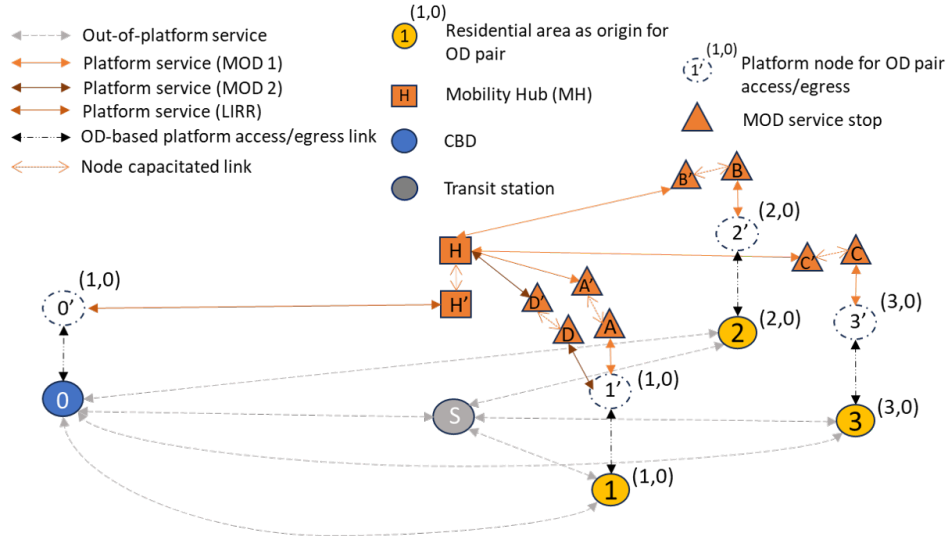


Figure 2: Toy network illustration

chain $A - A' - H$ remains closed. This reflects the competitive dynamics of the market, where multiple services may be available but not all are viable for platform operation.

The platform access fees for OD (1, 0) and (2, 0) are set at 8.49 and 6.84, respectively, to maximize total revenue. To incentivize operators to participate in the platform without incurring losses, the operator receives a subsidy of 3.50 per traveler entering the service at node D for OD (1, 0). For OD pair (2, 0), the corresponding operator subsidy is 4.50. This indicates that involving operators in the route from service node B to hub H is more costly for the platform. For nodes A and C, other modes dominate the options. Therefore, no subsidy is offered, as opening services at these nodes is deemed unprofitable.

For OD (3, 0), the direct link in the dummy subnetwork dominates all other options. Even if the platform were to offer free access to the MOD service link (C,H), travelers would not choose it, nor would the operator serve that area. Due to the overall low usage of MaaS services in this scenario, the hub is significantly underutilized, operating at only 21.59% of its maximum capacity. The total platform service profit in this case is \$161.10.

4.2. LIRR mobility hubs case study

We further use three LIRR stations: Ronkonkoma, St. James, and Sayville, and their surrounding neighborhoods, represented by travel analysis zones (TAZs), to test the proposed model. These three stations are treated as candidate mobility hubs. We use the centroids of census tracts within a 5-mile radius of each station as origin nodes, with Manhattan as the destination for a typical weekday morning AM period. In total, 78 neighborhoods are covered. Two layers of subnetworks are defined, similar to the toy network. **Fig. 3** illustrates the platform subnetwork. Each service node is directly connected via MOD service links, with candidate mobility hubs established at each LIRR station. We assume these primary MOD services are managed by a single operator. To model market competition similar to the toy network, we introduce a second MOD service provider in the vicinity of Ronkonkoma station. This secondary operator functions within a 3-mile radius, covering 20 neighborhoods. In a real world context, the primary MOD service (MOD 1) represents larger scale microtransit options, such as ride hailing or ridepooling. For example, Suffolk County operates an on-demand service

Table 2: Network Input and Parameters

Source	Sink	c_1^t (\$)	c_1^o (\$)	\hat{p}_1 (\$)	d_l
1	0	9	0	N/A	4
2	0	9	0	N/A	4
3	0	9	0	N/A	4
1	1'	0	0	10	0.1
2	2'	0	0	10	0.1
3	3'	0	0	10	0.1
1'	A	0	0	N/A	0.1
1'	D	0	0	N/A	0.1
2'	B	0	0	N/A	0.1
3'	C	0	0	N/A	0.1
A'	H	5	2	N/A	1
B'	H	5	2	N/A	2
C'	H	5	2	N/A	3
D'	H	3	3	N/A	1
1	S	7	0	N/A	1
2	S	7	0	N/A	2
3	S	7	0	N/A	3
H'	0'	6	0	N/A	4
S	0	7	0	N/A	4
Maximum hub capacity, b_l					200
Maximum service node capacity, z_l					50
Maximum subsidy allowed per traveler, \hat{r}_l					5
α_1, α_2					1, 0.5
Capacity cost, c_i					1

Table 3: Comparison of link prices, subsidies and flows across base and alternative scenarios

Link	OD Pair s	Price, p_l	Subsidy, r_l	Flow, $x_{l,s}q_s$
(1, 0)	(1, 0)	N/A	N/A	32.87
(2, 0)	(2, 0)	N/A	N/A	82.59
(3, 0)	(3, 0)	N/A	N/A	100
(1, 1')	(1, 0)	8.49	N/A	30.82
(1', D)	(1, 0)	N/A	3.5	30.82
(D', H)	(1, 0)	N/A	N/A	30.82
(H', 0)	(1, 0)	N/A	N/A	30.82
(2, 2')	(2, 0)	6.84	N/A	12.35
(2, B)	(2, 0)	N/A	4.5	12.35
(B', H)	(2, 0)	N/A	N/A	12.35
(H', 0)	(2, 0)	N/A	N/A	12.35
(1, S)	(1, 0)	N/A	N/A	36.30
(S, 0)	(1, 0)	N/A	N/A	36.30
(2, S)	(2, 0)	N/A	N/A	5.06
(S, 0)	(2, 0)	N/A	N/A	5.06
Hub Capacity, v_i		21.59%		
Objective value, Φ_0		\$161.10		

in Southampton that provides last mile access to the LIRR Southampton station and the S92 bus (Southampton, 2026). The localized MOD service (MOD 2) represents micromobility solutions, such as bike sharing or shared scooters. The resulting network comprises 98 service nodes connected by 133 direct microtransit service links. Additionally, three LIRR links are included to represent line-haul services.

For the dummy subnetwork, 78 direct service links parallel to the MOD links are added to represent other access services. Another 78 direct links from service nodes to the Manhattan node are also included in the dummy subnetwork. As a result, the whole network has 380 nodes and 642 links serving the 78 OD pairs. By comparison, the expanded Sioux Falls network in Liu and Chow (2024) has 30 OD pairs, 82 nodes, and 748 links.

The 78 OD pairs, each originating from a service node to Manhattan, have demand simulated from a normal distribution with a mean of 60 and a standard deviation of 20, representing a typical weekday AM period (see **Table. A1** in Appendix for details). The simulated total demand is 4,734, with an average being 60.69 per census tract OD pair. Note that this level of demand falls in the range of observation, as Ronkonkoma Station, the largest one, has 5,452 free parking spaces for general passengers, and fills up on a typical weekday.

Each MOD service node is assigned a capacity of 50, while the Mobility Hub (MH) has a capacity of 2,000. The maximum platform access fee (which includes the LIRR ride) is capped at \$30, and the operator subsidy is limited to a maximum of \$5 per traveler. α_1 and α_2 are set to be 1 and 0.5, respectively. Other input elements are summarized in **Table 4**. The interpretation of the \hat{p}_l parameter varies depending on the link type. For MOD platform access links, it represents the price cap. Conversely, for dummy network links, it represents the fixed fee paid by travelers. \bar{d}_l represents the average link length. To reflect the trade-off

between micromobility and microtransit, MOD 2 is modeled with lower operating costs but slower service speeds than MOD 1.

For the experimental design, we first establish two baseline scenarios: one without the proposed platform ("business as usual") by solving the lower level problem without the platform subnetwork, and a second with the proposed platform by solving the problem with the stated network and input variables to determine the baseline objective value. We then perform a sensitivity analysis focusing on MOD operating costs within the platform network and driving costs within the dummy network to illustrate the sensitivities captured by the model. To further evaluate system dynamics, we then analyze three targeted scenarios: (1) eliminating micromobility links to assess operator participation effects; (2) removing the Ronkonkoma Mobility Hub designation to quantify its added value; and (3) reducing the operator subsidy cap to \$3 to examine the impact of tighter fiscal constraints on planning decisions.

All cases are run on a device with an Intel(R) i7-13705 processor. We initiate the proposed algorithm with ρ_0 equal to 300 and terminate the algorithm either after 10 iterations or when the optimality gap is below 0.1%. Each iteration has a runtime limit of 10 minutes.

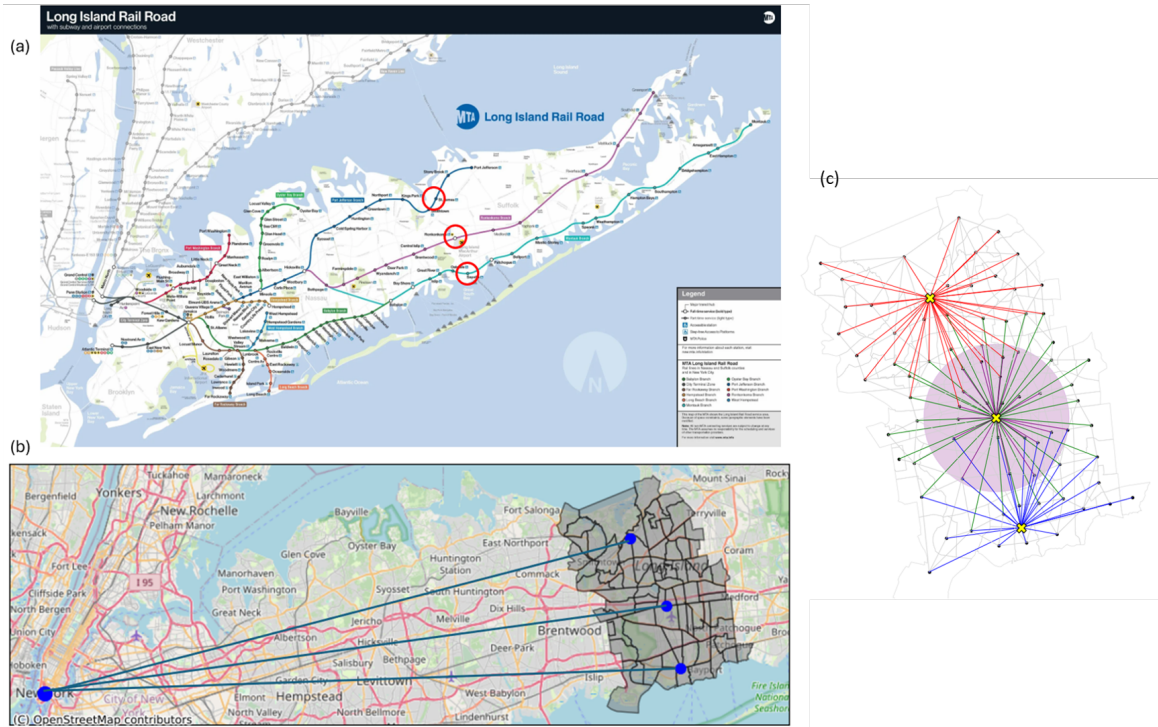


Figure 3: LIRR network illustration: (a) map of LIRR from the MTA with the three stations circled in red; (b) overlay of the census tracts within 5 miles of those stations; and (c) the MaaS subnetwork with links connecting each census tract to nearby stations

4.2.1. Base case

Prior to solving the full bilevel model, we solved the lower-level model exclusively on the dummy network to establish traveler behavior in the absence of platform participation. Using the parameters listed in **Table 4**, we observe a mode split where 64.52% of travelers utilize the existing transit network and 35.45% opt for direct driving. The lower level objective value is

Table 4: Subnetwork Mode Parameters

Subnetwork	Mode	c_1^t (\$)	c_1^o (\$)	\hat{p}_1 (\$)	\bar{d}_1 (miles)
MOD	Access	0	0	20	0.1
	MOD 1	0.42	0.5	0	3
	MOD 2	0.5	0.3	0	1.8
	LIRR	1.2	0	0	25
Dummy	LIRR dummy	1.30	0	20	25
	Drive	1.33	0	21	30
	Park-n-Ride	0.5	0	0	5

5,451.97. These results serve as a "business as usual" baseline for comparison with the proposed bilevel model, allowing us to quantify the impact of introducing the platform service.

We then run the full bilevel model with the platform network added. The proposed algorithm finds a solution with an optimality gap of less than 1% in 3092 seconds. The runtime is significantly shorter than other link-based MaaS design models proposed by previous studies (Liu and Chow, 2024; Yao and Zhang, 2024) when solving problems with similar scale. In comparison, the Sioux-Fall network-based case described in Liu and Chow (2024) requires longer than a 4-hour run time to converge. This illustrates the scalability of the proposed algorithm in real-world applications.

To demonstrate convergence to the global optimum, we solved the model across a range of ρ values. We then fix the upper-level decision variables to their corresponding optimal outputs and solved the lower-level model directly. Using the resulting flows and capacities, we calculated the actual platform profit. As illustrated in **Fig. 4**, both values converge as ρ increases. However, the rate of convergence diminishes as ρ approaches a critical value. Once ρ exceeds this threshold, the optimum of the single-level formulation effectively represents the true global optimum of the bilevel model. Future studies could focus on developing algorithms that efficiently identify this critical threshold to further accelerate the solution process.

The final solution has platform access prices (which includes the access mode and LIRR) ranging from \$22.47 to \$30, and the general distribution can be observed in **Fig. 6(a)**. This pricing structure is economically reasonable when compared to general LIRR commuting costs, ensuring the platform remains a viable option for travelers. The total profit from the MOD service is \$38721.23, and 35.32% (1,661 passengers) of the total OD demand uses the MH centered platform. 741 people use service based at Ronkonkoma station, 550 use service based at St. James station, and 380 use service based at Sayville. **Fig. 5** illustrates the percent mode share of the MOD services across the 78 neighborhoods.

The operator subsidy ranges from \$0 to \$5. However, the distribution is polarized, with most values falling either below \$1 or above \$4, as illustrated in **Fig. 6(b)**. This indicates that the platform strategically concentrates financial incentives on specific, high-priority service links rather than distributing them uniformly. We observe a strong positive correlation of 0.66 between operator subsidies and passenger flow. This suggests that the platform allocates higher per-traveler subsidies to high-demand links to ensure that the total subsidy volume is sufficient to cover the operator's aggregate costs. Conversely, the correlation between link length and subsidy level is weakly positive, at 0.11. While areas further from MHs generally require higher subsidies to be viable, distance alone is not the sole determinant. Areas easily accessible via

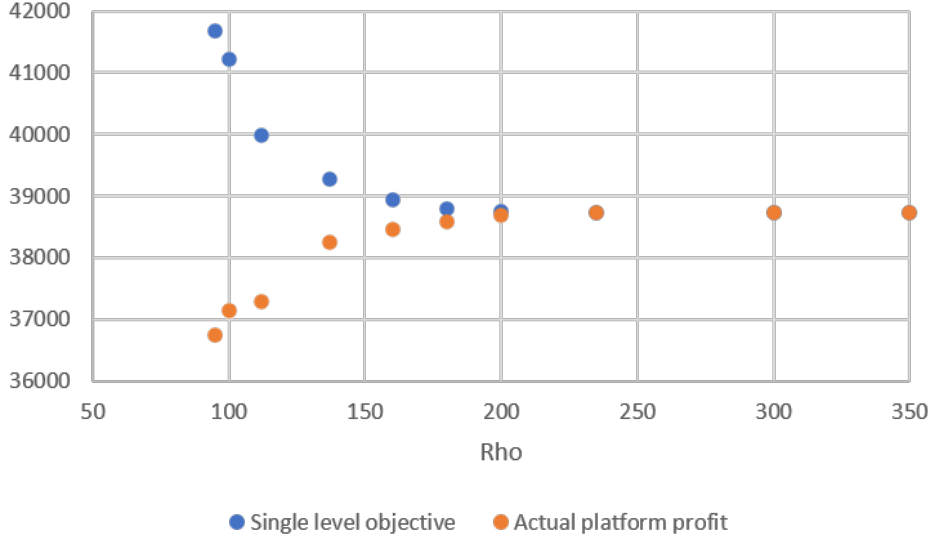


Figure 4: Convergence between single level objective and true platform profit.

the dummy network often have lower platform usage. Furthermore, variations in access fees create different passenger flows for areas at similar distances. Consequently, the relationship between distance and subsidy is only weakly correlated.

Both the major operator (MOD 1 in **Table 2**) and the smaller operator receive the subsidies to reach break even. The major operator incurs \$4781.41 in operating costs for the in-platform service and receives an equivalent \$4781.41 in subsidies, and the smaller operator incurs \$220.76 in operating costs and receives \$220.76 from the platform. With the introduction of the platform service, the mode share of direct driving drops to 22.46%, representing a 36.6% decrease compared to the no-platform scenario. To quantify the utility impact, we compared the lower-level objective values of both models. The objective value decreases from 5,451.97 in the baseline (dummy network only) scenario to 5,154.90 in the optimal platform case. Since the lower-level objective measures user disutility, this reduction demonstrates the platform’s positive impact on overall system welfare. Per Remark 1, this particular baseline suggests there is an opportunity for a subsidy-enabled MH platform to serve this market.

Remark 1. The model identifies an opportunity for a MH platform when it reduces the overall travel disutilities with a fare bundle that can cover the costs of all participating operators.

We subsequently conducted two sensitivity analyses focusing on cost-related components: the MOD link operating cost and the direct driving cost. These analyses reveal how fluctuations in these costs impact both the platform’s profitability and the utilization of the three MHs.

MOD link operating cost sensitivity analysis.

We first perform a sensitivity analysis on the operating costs of MOD links. We varied the operating costs for services operated by both MOD 1 and MOD 2 across a range of -50% to +50%. **Fig. 7** illustrates the relationship between these operating costs and the platform profit. As operating costs rise, the platform is required to provide higher subsidies. This leads to an increase in the platform access fee, as shown in **Table. 5**, which subsequently reduces platform

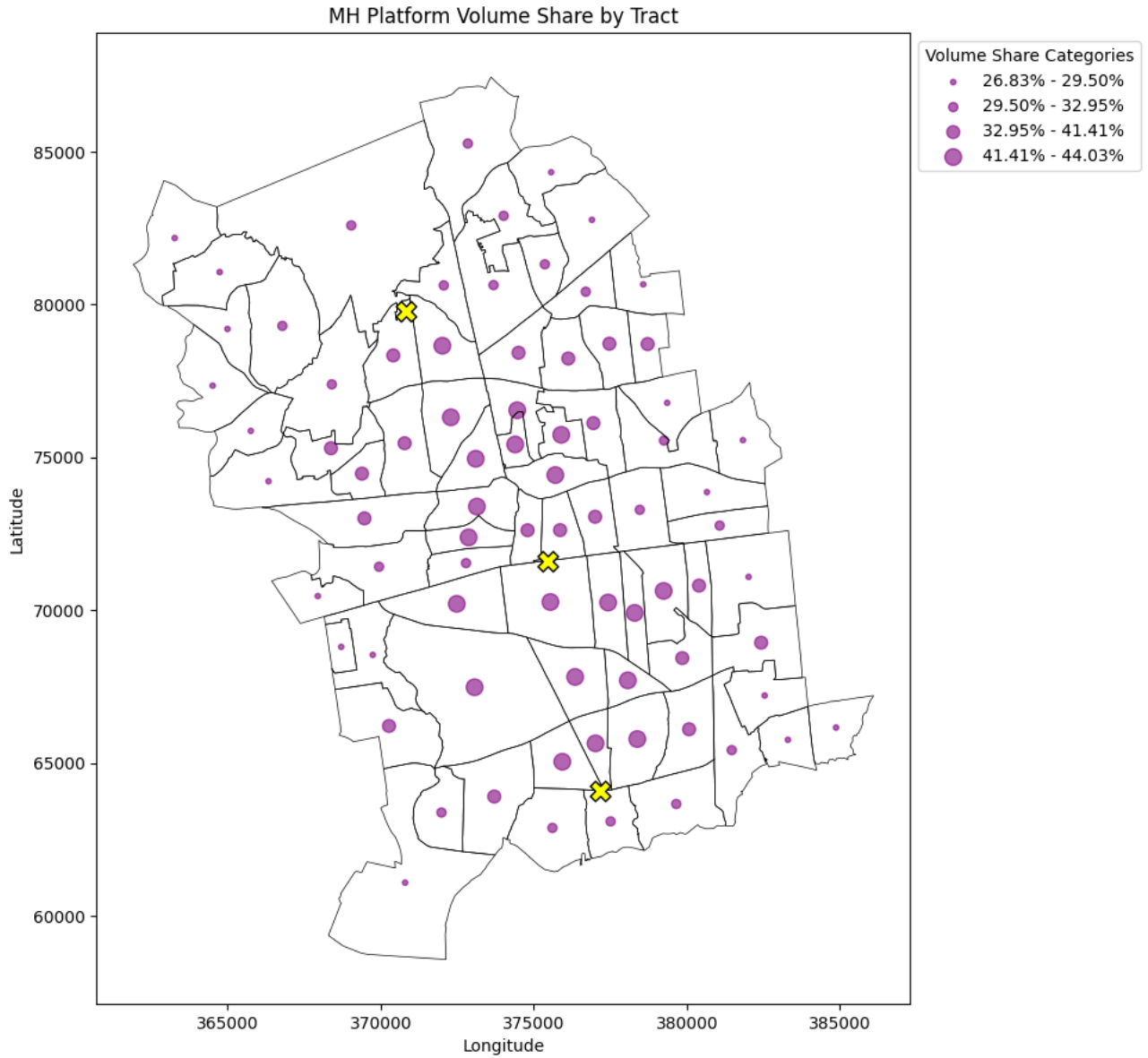


Figure 5: Mode share of MH based MOD services.

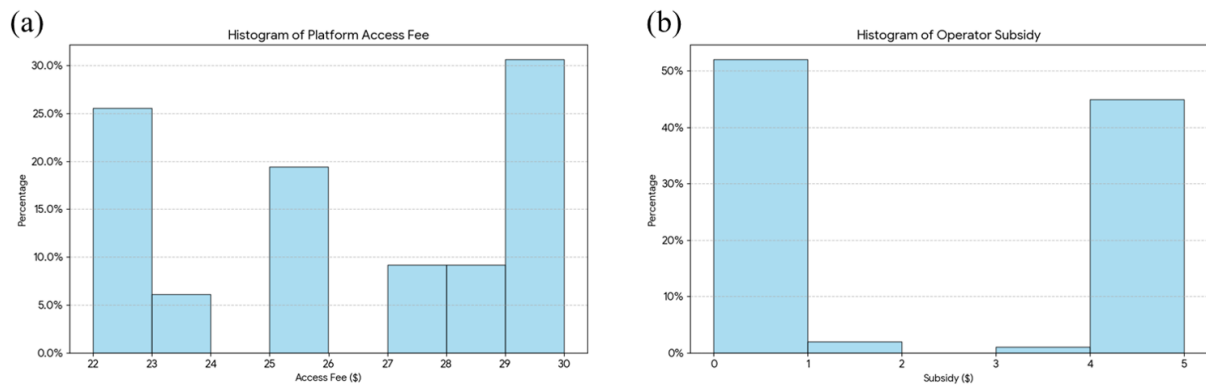


Figure 6: Histogram of (a) platform access fee and (b) histogram of operator subsidy.

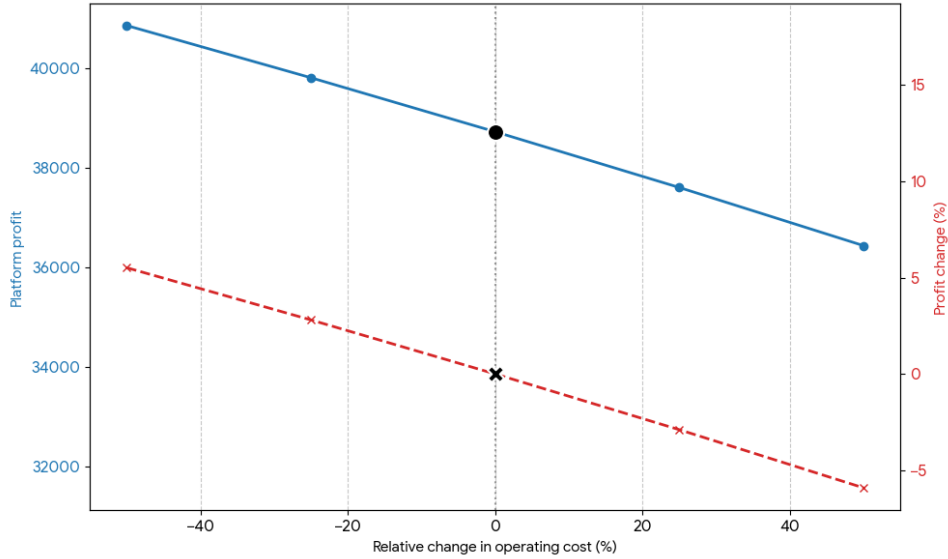


Figure 7: Relationship between platform profit and MOD link operating cost

Table 5: Impact of operating cost changes on access fee and share of platform usage

Operating Cost Change (%)	Average Access Fee	Relative Fee Change (%)	Share (%) of MH usage
-50	26.13	-1.94	36.14
-25	26.37	-1.06	35.79
0	26.65	0.00	35.32
+25	26.92	1.01	34.82
+50	27.16	1.93	34.30

service usage (and vice versa). Notably, we observed a linear relationship between operating costs and platform profit. A 50% fluctuation in operating cost results in a 5% shift in platform profit under these baseline settings. Given that the subsidy comprises only 13% of the total platform revenue in the base scenario, even a 50% variation in cost leads to only a marginal adjustment in the platform access fee.

Fig. 8 illustrates the relationship between link operating costs and the volumes across the three MH locations. While the volumes at all three hubs exhibit a consistent inverse relationship with operating costs, the response is asymmetric. The negative impact of a cost increase is stronger than the positive gain from a cost reduction. Specifically, a 50% decrease in operating cost increases hub volumes by 2% to 2.5%, with St. James benefiting the most. However, a 50% cost surge leads to a sharper decline of 3.0%, with Ronkonkoma becoming the most impacted. This suggests that while lower costs encourage some additional usage, higher costs penalize demand more severely.

Direct driving cost sensitivity analysis.

We subsequently perform a sensitivity analysis on direct driving costs to evaluate the impact of competing mode pricing. Fig. 9 illustrates the resulting relationship. Since private driving functions as a substitute mode, increasing its cost dissuades travelers from using private vehicles. This drives higher demand for MH services and increases platform profit. For instance, a 43%

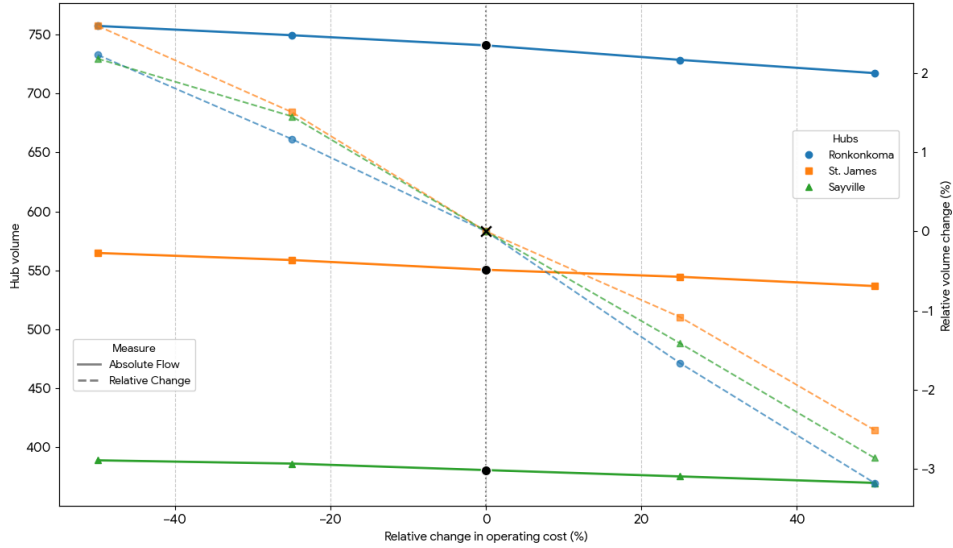


Figure 8: Relationship between MH usage and MOD link operating cost

increase in driving costs, which is comparable to a \$9 congestion toll for entering New York City, results in a 16% gain in platform profit. Consistent with our operating cost analysis, the relationship between platform profit and driving cost changes is linear. Table. 6 details the corresponding shifts in access fees and the platform’s overall mode share. Notably, the platform access fee covaries positively with driving costs. As driving becomes more expensive, the platform strategically raises its access fee to capitalize on the influx of deterred drivers. This creates an indirect effect where travel becomes universally more expensive, negatively impacting travelers who rely on the platform as an alternative to driving.

Table 6: Impact of driving cost changes on access fee and platform mode share

Driving Cost Change (%)	Avg. Access Fee	Relative Fee Change (%)	Mode Share (%)
-52	24.59	-7.72	31.66
-43	25.00	-6.17	32.27
-33	25.42	-4.63	32.88
-24	25.83	-3.08	33.48
-14	26.19	-1.71	34.17
0	26.65	0.00	35.32
10	26.93	1.06	36.10
19	27.21	2.11	36.89
29	27.49	3.16	37.68
43	27.88	4.60	38.90

Fig. 10 illustrates the relationship between direct driving costs and traffic volumes across the three MH locations. When driving costs decrease, the relative decline in volume is nearly identical across all three hubs. However, as driving costs rise, the relative growth rates begin to diverge slightly. St. James exhibits the greatest relative gain, while Ronkonkoma shows the lowest. Despite this minor divergence, the three hubs demonstrate broadly similar demand

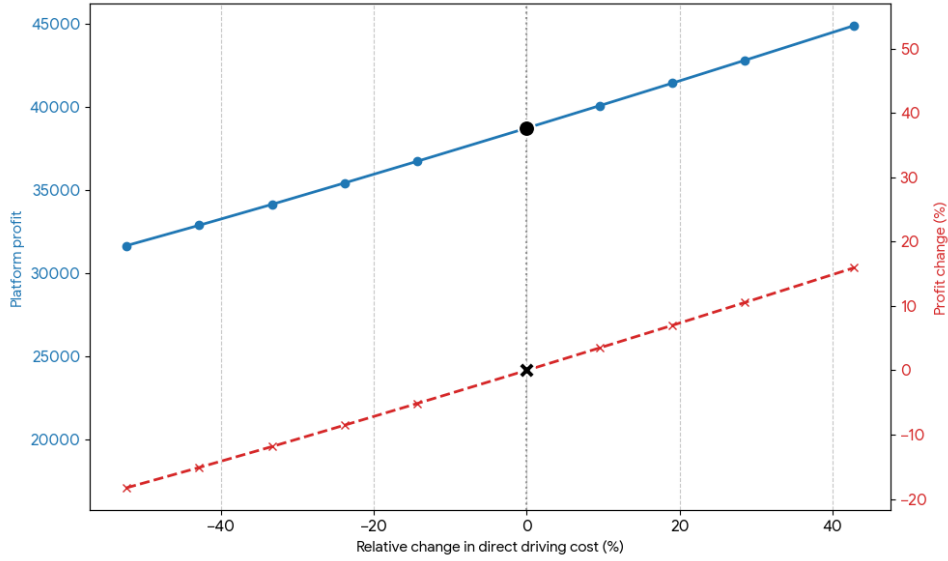


Figure 9: Relationship between platform profit and direct driving cost

elasticity with respect to driving costs. Consequently, policy measures that change the cost of driving would likely produce a consistent impact on ridership across the three hubs.

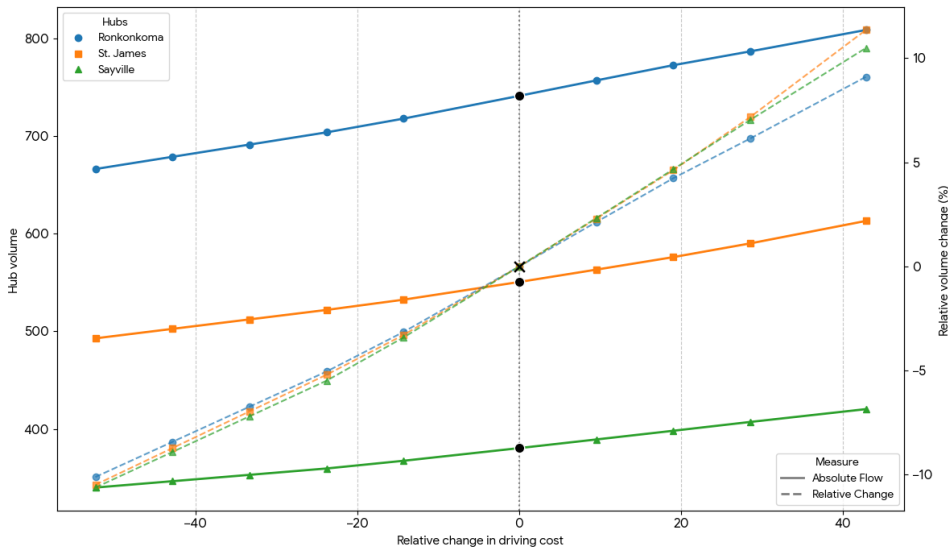


Figure 10: Relationship between MH usage and direct driving cost

4.2.2. Evaluating the impact of in-platform service competition

To examine the impact of reduced operator competition, we eliminated MOD 2 service entirely. This consolidation resulted in a 0.73% decline in total platform profit (\$38,439.05) and a marginal 0.1% drop in ridership (1,659 passengers). While the average platform access fee remained relatively stable (increasing from \$26.65 to \$26.72), the pricing distribution shifted significantly. The first quartile rose from \$22.95 to \$25.29, and the median increased from

\$25.86 to \$27.88. This indicates that reduced competition disproportionately raised costs for lower-priced trips.

Due to the higher operating costs associated with the remaining operator, the total subsidy rises from \$5002.17 to \$5072.32, an increase of 1.40%. Therefore, incorporating more service options into the platform proves beneficial for both the platform and travelers. The platform can potentially reduce total subsidy costs, while travelers benefit from greater access and a wider range of choices within the platform ecosystem with lower access fee.

Remark 2. Reduced competition in participating access operators to the MH platform can disproportionately raise costs for travelers even as the impact to the platform's profits may be minimal.

4.2.3. Quantifying the value of an MH connecting microtransit to Ronkonkoma station

To quantify the value added of the MH at Ronkonkoma, we apply the same model to a network modification where the Ronkonkoma MH (the central hub in **Fig. 3**) and its associated MOD links are removed. Note that the Ronkonkoma station itself remains accessible within the dummy network. In this scenario, 63 MOD service nodes and 63 MOD links remain available on the MaaS platform, with only 15 census tracts losing platform service access.

Consequently, MaaS platform usage drops significantly from 35.32% in the baseline to 22.30%, with travelers diverting to the two remaining MHs or alternative out-of-platform modes. Total platform revenue contracts to \$24,311.86, implying that the inclusion of the Ronkonkoma MH generates an incremental value of \$14,409.37 per AM peak period. Despite these volume shifts, the pricing structure remains stable. Average access fees change by less than 1%, with the first quartile shifting slightly from \$22.95 to \$23.38 and the median remaining virtually unchanged (\$25.86 vs. \$25.84).

Remark 3. Because the lower-level model is a coalitional choice model, the change in objective value for removing a MH captures the social surplus value of the MH that travelers and operators are collectively willing to pay for, i.e. the compensating variation of the MH location alternative.

4.2.4. Lower subsidy cap provided by platform

We reduce the subsidy cap from \$5 to \$3 while keeping the original network structure to evaluate the impact of subsidy constraints on platform planning decisions. The platform profit declines to \$37,746.32, representing a 2.52% decrease compared to the baseline scenario, while the total number of travelers using the platform drops by 0.57% to 1652. Although the average access fee remains relatively stable with marginally decreasing by 1.16% to \$26.34, the allocation of subsidies shifts drastically. The total subsidy allocated to the two operators amounts to \$4,902.63 with high consolidation towards the major operator. MOD 1 sees a 1% increase in subsidy allocation with \$4,829.37, while the smaller MOD 2 faces a significant reduction of 66.81% to receiving only \$73.26. A sharp cut in subsidies caused MOD 2 ridership to fall from 149 to 42 and to only serve 15 out of the 20 covered areas, pushing the operator to the brink of market exit.

This drastic shift indicates that when subsidy flexibility is capped, the platform creates a "flight to quality", prioritizing the major operator (MOD 1) to secure core network capacity. The smaller operator (MOD 2), which provides a cheaper but slightly inferior service, likely relies on higher marginal incentives to keep operating. When the subsidy cap prevents the platform from bridging that gap, the platform effectively abandons the niche operator to preserve

the financial viability of the primary fleet. Consequently, the restrictive cap reduces overall service diversity and accessibility, leading to a net loss in platform access and profitability. These results further reinforce the importance of model analysis of operating policies surrounding MHs, as the impacts may not be easily predicted.

Remark 4. Restrictive subsidy caps can impact different operators disproportionately.

5. Conclusion

In this study, we propose a MH platform design model addressing both the theoretical and computational gaps identified in recent literature for both MaaS and mobility hub based applications. While previous research has largely emphasized the role of MHs as physical transfer points or focused solely on optimal facility location, our approach extends the function of MHs to include their strategic influence on both operator and traveler decision-making, particularly through the explicit modeling of pricing structures and targeted subsidies. By leveraging the PURC framework within a bilevel optimization structure, we capture the complex interplay between public platforms and private mobility operators while also ensuring computational scalability necessary for real-world, large-scale applications.

The proposed model integrates the joint operational planning between travelers and operators, which is essential for effective MaaS platform deployment, while also capturing the competitive dynamics of multiple operator participation. The framework utilizes a bilevel structure: a revenue-maximizing upper level, where the platform determines optimal traveler-facing pricing and operator-facing subsidy allocation strategies. A convex quadratic lower level, where travelers and operators jointly optimize flows and capacities. We transform this bilevel formulation into a single-level problem using KKT conditions, guaranteeing the existence of a global optimum. Furthermore, an augmented penalty-based algorithm is proposed to enhance computational tractability and reduce runtime.

We demonstrate the model application through two sets of numerical examples. The toy example demonstrates the effectiveness of the proposed model and validates the existence of a global optimum. The results show that the model can optimally allocate link-specific resources from a revenue-maximization perspective. We further test the model on a larger network based on LIRR stations and their service areas. A total of 380 nodes and 642 links are involved in the base network with 78 OD pairs. Several insights are obtained through the tests:

- The proposed model is much more scalable compared to similar platform design models in past studies. Similar-sized problems require hours of runtime ((Liu and Chow, 2024; Yao and Zhang, 2024)), while ours takes less than 1 hour when setting the right conditions.
- Platform profit exhibits a linear relationship with both MOD link operating costs and direct driving costs within the analyzed network configuration.
- The platform’s profitability demonstrates greater sensitivity to changes in direct driving costs than to changes in MOD service operating costs.
- All three MHs demonstrate similar level of ridership shifts when subjected to variations in service operating and driving costs.
- Market competition is important in reducing both the overall subsidy level and platform access pricing, specifically when the operators control different levels of market power.

- The use of the PURC-based lower-level problem allows policymakers to quantify the social surplus value of a MH, and to determine how to control subsidies to encourage platform service participation and traveler access.

The proposed model can be applied to more complex MaaS service designs involving more operators. With more operators, subsidy schemes based on setting a rate per operator can be done. Heterogeneous travel groups can be considered (e.g. splitting each OD pair into portions by income group). The proposed model is sensitive to changes in network topology, a common feature in existing service design problems. When different spatial aggregations are used to construct the network, associated parameters, including link travel times, operating costs, and coefficients such as α_1 and α_2 , must be adjusted and recalibrated accordingly. Therefore, proper network construction using accurate observational data is an essential prerequisite. In future studies, we aim to incorporate supply-side functions that reflect operational performance into the bi-level model. This would relax the current assumption of fixed supply-side costs, allowing the model to determine optimal operator strategies corresponding to the platform’s planning decisions.

There are multiple gaps remaining. Congestion effects on out-of-platform links can also be added. The link-additive approach could negate non link-additive factors impacting traveler and operator choices. Competition between platforms can be considered by changing the upper level into a generalized Nash equilibrium. Alternative applications of mobility hubs can be studied using this framework: urban air mobility and freight distribution, for example. The model can be further expanded to three-sided markets to deal with electric charging integration.

Acknowledgments

The project is funded by the National Science Foundation (NSF) CMMI-2423908.

References

- Amsterdam (2025). ehubs – smart shared green mobility hubs. <https://www.nweurope.eu/projects/project-search/ehubs-smart-shared-green-mobility-hubs/>. Interreg North-West Europe. Accessed 2025-06-20.
- Arias-Molinares, D., Xu, Y., Büttner, B., and Duran-Rodas, D. (2023). Exploring key spatial determinants for mobility hub placement based on micromobility ridership. *Journal of Transport Geography*, 110:103621.
- Arnold, T., Frost, M., Timmis, A., Dale, S., and Ison, S. (2023). Mobility hubs: Review and future research direction. *Transportation Research Record*, 2677(2):858–868.
- Aydin, N., Seker, S., and Özkan, B. (2022). Planning location of mobility hub for sustainable urban mobility. *Sustainable Cities and Society*, 81:103843.
- Bandiera, C., Connors, R. D., and Viti, F. (2024). Mobility service providers’ interacting strategies under multi-modal equilibrium. *Transportation Research Part C: Emerging Technologies*, 168:104766.

- Banerjee, S., Kabir, M. M., Khadem, N. K., and Chavis, C. (2020). Optimal locations for bike-share stations: A new gis based spatial approach. *Transportation Research Interdisciplinary Perspectives*, 4:100101.
- Bell, M. G. (1995). Stochastic user equilibrium assignment in networks with queues. *Transportation Research Part B: Methodological*, 29(2):125–137.
- Bertsimas, D., Sian Ng, Y., and Yan, J. (2020). Joint frequency-setting and pricing optimization on multimodal transit networks at scale. *Transportation Science*, 54(3):839–853.
- Caggiani, L., Camporeale, R., Dimitrijević, B., and Vidović, M. (2020a). An approach to modeling bike-sharing systems based on spatial equity concept. *Transportation Research Procedia*, 45:185–192.
- Caggiani, L., Colovic, A., and Ottomanelli, M. (2020b). An equality-based model for bike-sharing stations location in bicycle-public transport multimodal mobility. *Transportation Research Part A: Policy and Practice*, 140:251–265.
- Chen, R. B. and Valant, C. (2023). Stability and convergence in matching processes for shared mobility systems. *Networks and Spatial Economics*, 23(2):469–486.
- Dempe, S. (2002). *Foundations of bilevel programming*. Springer.
- Djavadian, S. and Chow, J. Y. (2017). An agent-based day-to-day adjustment process for modeling ‘mobility as a service’ with a two-sided flexible transport market. *Transportation research part B: methodological*, 104:36–57.
- Duran-Rodas, D., Wright, B., Pereira, F. C., and Wulfhorst, G. (2021). Demand and/or equity (dare) method for planning bike-sharing. *Transportation Research Part D: Transport and Environment*, 97:102914.
- Fosgerau, M., Paulsen, M., and Rasmussen, T. K. (2022). A perturbed utility route choice model. *Transportation Research Part C: Emerging Technologies*, 136:103514.
- Frank, L., Dirks, N., and Walther, G. (2021). Improving rural accessibility by locating multimodal mobility hubs. *Journal of transport geography*, 94:103111.
- Grigolon, A., Garritsen, K., and Geurs, K. (2025). Willingness to pay for shared mobility hubs: a stated choice joint-survey in four european cities. *Networks and Spatial Economics*, pages 1–22.
- Hörcher, D. and Graham, D. J. (2020). Maas economics: Should we fight car ownership with subscriptions to alternative modes. *Economics of Transportation*, 22(100167):10–1016.
- Huang, W., Jian, S., and Rey, D. (2024). Non-additive network pricing with non-cooperative mobility service providers. *European Journal of Operational Research*, 318(3):802–824.
- Karbaumer, R. and Weltring, W. (2025). Was sind mobil.punkte? <https://mobilpunkt-bremen.de/mobil-punkte/>. mobil.punkt Bremen. Accessed 2025-06-20.

- Liu, B. and Chow, J. Y. J. (2024). On-demand mobility-as-a-service platform assignment games with guaranteed stable outcomes. *Transportation Research Part B: Methodological*, 188:103060.
- Liu, B., Watling, D., and Chow, J. Y. (2025). Stochastic assignment games for mobility-as-a-service markets. *arXiv preprint arXiv:2512.19328*.
- Ma, T.-Y., Rasulkhani, S., Chow, J. Y. J., and Klein, S. (2019). A dynamic ridesharing dispatch and idle vehicle repositioning strategy with integrated transit transfers. *Transportation Research Part E: Logistics and Transportation Review*, 128:417–442.
- Marcotte, P. and Zhu, D. L. (1996). Exact and inexact penalty methods for the generalized bilevel programming problem. *Mathematical Programming*, 74:141–157.
- Miramontes, M., Pfertner, M., Rayaprolu, H. S., Schreiner, M., and Wulfhorst, G. (2017). Impacts of a multimodal mobility service on travel behavior and preferences: user insights from munich’s first mobility station. *Transportation*, 44:1325–1342.
- Nair, R. and Miller-Hooks, E. (2014). Equilibrium network design of shared-vehicle systems. *European Journal of Operational Research*, 235(1):47–61.
- Ouyang, Y. and Yang, H. (2023). Measurement and mitigation of the “wild goose chase” phenomenon in taxi services. *Transportation Research Part B: Methodological*, 167:217–234.
- Pantelidis, T. P., Chow, J. Y., and Rasulkhani, S. (2020). A many-to-many assignment game and stable outcome algorithm to evaluate collaborative mobility-as-a-service platforms. *Transportation Research Part B: Methodological*, 140:79–100.
- Petrović, M., Josip Mlinarić, T., and Šemanjski, I. (2019). Location planning approach for intermodal terminals in urban and suburban rail transport. *Promet-Traffic&Transportation*, 31(1):101–111.
- Pinto, H. K., Hyland, M. F., Mahmassani, H. S., and Verbas, I. Ö. (2020). Joint design of multimodal transit networks and shared autonomous mobility fleets. *Transportation Research Part C: Emerging Technologies*, 113:2–20.
- Prato, C. G. (2009). Route choice modeling: past, present and future research directions. *Journal of choice modelling*, 2(1):65–100.
- Rasulkhani, S. and Chow, J. Y. (2019). Route-cost-assignment with joint user and operator behavior as a many-to-one stable matching assignment game. *Transportation Research Part B: Methodological*, 124:60–81.
- Ren, X. and Chow, J. Y. (2025). A data fusion approach for mobility hub impact assessment and location selection: integrating hub usage data into a large-scale mode choice model. *arXiv preprint arXiv:2510.08366*.
- Sinha, A., Malo, P., and Deb, K. (2017). A review on bilevel optimization: From classical to evolutionary approaches and applications. *IEEE transactions on evolutionary computation*, 22(2):276–295.

- Southampton (2026). Suffolk transit on-demand. <https://www.southamptontownny.gov/1618/Suffolk-Transit-On-Demand>.
- van den Berg, V. A., Meurs, H., and Verhoef, E. T. (2022). Business models for mobility as a service (maas). *Transportation Research Part B: Methodological*, 157:203–229.
- Weustenenk, A. G. and Mingardo, G. (2023). Towards a typology of mobility hubs. *Journal of Transport Geography*, 106:103514.
- Xanthopoulos, S., van der Tuin, M., Azadeh, S. S., de Almeida Correia, G. H., van Oort, N., and Snelder, M. (2024). Optimization of the location and capacity of shared multimodal mobility hubs to maximize travel utility in urban areas. *Transportation Research Part A: Policy and Practice*, 179:103934.
- Xi, H., Aussel, D., Liu, W., Waller, S. T., and Rey, D. (2024a). Single-leader multi-follower games for the regulation of two-sided mobility-as-a-service markets. *European Journal of Operational Research*, 317(3):718–736.
- Xi, H., Li, M., Hensher, D. A., Xie, C., Gu, Z., and Zheng, Y. (2024b). Strategizing sustainability and profitability in electric mobility-as-a-service (e-maas) ecosystems with carbon incentives: A multi-leader multi-follower game. *Transportation Research Part C: Emerging Technologies*, 166:104758.
- Yao, R. and Zhang, K. (2024). Design an intermediary mobility-as-a-service (maas) platform using many-to-many stable matching framework. *Transportation Research Part B: Methodological*, page 102991.
- Zhang, W., Honnappa, H., and Ukkusuri, S. V. (2020). Modeling urban taxi services with e-hailings: A queueing network approach. *Transportation Research Part C: Emerging Technologies*, 113:332–349.

Appendix

Table A1: Simulated Demand Data

Origin (Census Tract)	Destination	Demand
3610300134704	NYC	37
3610300134902	NYC	75
3610300134903	NYC	50
3610300134904	NYC	72
3610300134906	NYC	44
3610300134907	NYC	56
3610300135002	NYC	76
3610300135003	NYC	57
3610300135004	NYC	65

Continued on next page

Origin (Census Tract)	Destination	Demand
3610300135005	NYC	31
3610300135104	NYC	60
3610300135301	NYC	52
3610300135303	NYC	87
3610300135304	NYC	97
3610300135401	NYC	46
3610300135402	NYC	35
3610300135403	NYC	83
3610300145704	NYC	47
3610300145803	NYC	41
3610300145804	NYC	90
3610300145805	NYC	64
3610300145807	NYC	78
3610300145808	NYC	52
3610300146402	NYC	83
3610300146403	NYC	83
3610300146404	NYC	72
3610300146604	NYC	53
3610300146605	NYC	49
3610300146606	NYC	58
3610300146607	NYC	62
3610300146608	NYC	40
3610300146611	NYC	67
3610300146612	NYC	42
3610300146613	NYC	109
3610300146614	NYC	67
3610300146615	NYC	64
3610300147503	NYC	72
3610300147601	NYC	87
3610300147602	NYC	58
3610300147701	NYC	47
3610300147702	NYC	28
3610300147802	NYC	63
3610300147803	NYC	47
3610300147804	NYC	57
3610300147901	NYC	58
3610300147902	NYC	44
3610300158002	NYC	76
3610300158006	NYC	72
3610300158007	NYC	29
3610300158009	NYC	33
3610300158010	NYC	51
3610300158011	NYC	29

Continued on next page

Origin (Census Tract)	Destination	Demand
3610300158103	NYC	72
3610300158104	NYC	48
3610300158107	NYC	77
3610300158108	NYC	87
3610300158110	NYC	97
3610300158115	NYC	55
3610300158502	NYC	58
3610300158505	NYC	53
3610300158506	NYC	78
3610300158507	NYC	67
3610300158508	NYC	62
3610300158510	NYC	31
3610300158511	NYC	65
3610300158512	NYC	56
3610300158604	NYC	78
3610300158605	NYC	51
3610300158606	NYC	62
3610300158607	NYC	67
3610300158608	NYC	74
3610300158609	NYC	17
3610300158802	NYC	75
3610300158803	NYC	46
3610300158804	NYC	64
3610300158900	NYC	68
3610300159000	NYC	59
3610300159201	NYC	72
